

Ehrenfest time in the weak dynamical localization

C. Tian,¹ A. Kamenev,¹ and A. Larkin^{1,2,3}¹*Department of Physics, University of Minnesota, Minneapolis, Minnesota 55455, USA*²*William I. Fine Theoretical Physics Institute, University of Minnesota, Minneapolis, Minnesota 55455, USA*³*L. D. Landau Institute for Theoretical Physics, Moscow, 117940, Russia*

(Received 9 December 2004; revised manuscript received 15 April 2005; published 6 July 2005)

The quantum kicked rotor (QKR) is known to exhibit dynamical localization in the space of its angular momentum. The present paper is devoted to the systematic first-principles (without a regularizer) diagrammatic calculations of the weak-localization corrections for the QKR. Our particular emphasis is on the Ehrenfest time regime—the phenomena characteristic for the classical-to-quantum crossover of classically chaotic systems.

DOI: [10.1103/PhysRevB.72.045108](https://doi.org/10.1103/PhysRevB.72.045108)

PACS number(s): 05.45.-a, 42.50.Vk

I. INTRODUCTION

In recent years it has become abundantly clear that driven quantum systems exhibit behavior that is qualitatively different from their classical counterparts. Indeed, the average energy stored in a driven classically chaotic system linearly increases at a steady rate. In other words, such behavior may be characterized as a diffusion in the system's phase space. The remarkable feature of driven *quantum* systems is finiteness of their phase space motion (localization). Such dynamical localization phenomena were discussed in the context of pumped quantum dots,¹ ultracold atomic gases,^{2,3} or Bose-Einstein condensate⁴ subject to pulses of optical standing wave, optical microcavity,⁵ and other systems.

The simplest model that became a paradigm for studies of the quantum dynamical localization is quantum kicked rotor (QKR). It was numerical discovery of localization in QKR by Casati *et al.*^{6,7} in the late seventies that triggered the broad interest in the subject. Recent progress in trapping of cold atoms and optical manipulation with them led to experimental realization of the QKR with the unprecedented degree of control.^{2,4} The kicked rotor is described by the time-dependent Hamiltonian

$$\hat{H}(t) = \frac{\hat{p}^2}{2} + K \cos \hat{\theta} \sum_n \delta(t-n), \quad (1)$$

where angle $\hat{\theta}$ and angular momentum \hat{l} are the pair of canonically conjugated variables. The amplitude of the kicks is described by the dimensionless parameter K , also known as the classical stochasticity parameter. It is the only parameter of the corresponding classical problem. The quantum problem possesses another dimensionless parameter: the effective Planck constant \hbar . The latter enters the problem through the canonical commutation relation: $[\hat{\theta}, \hat{l}] = i\hbar$. The two parameters K and \hbar are straightforwardly related to the optical wavelength, amplitude, and atomic mass in cold atoms experiments.^{2,3,8}

Historically, the *classical* kicked rotor, or standard mapping, first introduced by Chirikov, served as the prototype model for various transport processes in plasmas.^{9,10} It was established that the classical dynamics of the kicked rotor exhibits complicated behavior. For a generic classical param-

eter K , stable and chaotic regions coexist in the phase space. The transition to the globally chaotic motion (with only isolated islands of the regular motion) takes place at sufficiently large K .^{9,10} In particular, for such large K the chaotic diffusion takes place in the space of angular momentum.^{9,10} The latter is associated with the unlimited diffusive expansion of an initially narrow momenta distribution: $\delta\langle l^2(t) \rangle = 2D_{cl}t$. The classical diffusion constant, D_{cl} , was a subject of numerous studies^{9,10} and is well understood by now.^{11,12} For large stochasticity parameter $K \gg 1$, one finds $D_{cl} \approx K^2/4 + O(K^{3/2})$, where the omitted corrections possess an oscillatory dependence on K .

The pioneering numerical studies of Casati *et al.*^{6,7} revealed that the corresponding *quantum* system, $\hbar \neq 0$, behaves in a dramatically different way. The initial diffusive expansion (that is, heating) saturates after a certain time, t_L . At later time the momentum distribution width stabilizes at $\delta\langle l^2(t) \rangle \sim \xi^2 = D_{cl}t_L$. It was soon suggested in Ref. 13 that similarly to Anderson localization, quantum phase interference may lead to the suppression of classical diffusion for long enough time. This heuristic idea was complemented by mapping the QKR onto a one-dimensional tight-binding Anderson model with the pseudorandom potential.^{13,14} Such interpretation leads to the estimate of the localization length as $\xi = D_{cl}/\hbar$, and thus $t_L = D_{cl}/\hbar^2$. The similarity was further confirmed by studies of a perturbation that breaks the “time-reversal symmetry” (TRS) of the QKR.¹⁵ Such perturbation suppresses the survival probability by a factor of 2. This is closely analogous to the doubling of the Anderson localization length by the static magnetic field, destroying the interference between a trajectory and its time-reversal partner.^{16,20}

If the momentum localization length, ξ , is much longer than the “microscopic” scale of the angular momentum (that is \hbar), then $K \gg \hbar$ and thus $t_L \gg 1$. In this case there is a parametrically long crossover regime from the classical diffusion: $\delta\langle l^2(t) \rangle \approx 2D_{cl}t$ for $1 < t \ll t_L$ to the strong localization: $\delta\langle l^2(t) \rangle = \xi^2$ for $t > t_L$. One may be able to develop a systematic perturbation theory in powers of $(t/t_L) \ll 1$, analogous to the weak-localization loop expansion in the Anderson localization theory.¹⁷ Such task was undertaken by Altland,¹⁸ who found for the one-loop correction: $\delta\langle l^2(t) \rangle = 2D_{cl}t(1 - 0.75\sqrt{t/t_L})$. It was suggested furthermore that the universal

long-time behavior of the QKR is described by the diffusive supersymmetric nonlinear σ model¹⁹ similar to those employed in the localization theory.²⁰

These calculations essentially map the QKR on a quantum particle in the field of a *white-noise* random potential. While such analogy is reasonable at long time scales $t \sim t_L \gg 1$, it fails to recognize details of the classical to quantum crossover at intermediate time scales. Indeed, a quantized classically chaotic system requires a certain time scale, called the Ehrenfest time, t_E , to develop quantum interference effects. This fact was realized independently in various contexts^{21,22} and nowadays is well documented in the literature.^{7,22–27} The physics behind this fact is as follows. To experience the quantum interference, two classical trajectories must converge to a region of the phase space of the size $\delta l \delta \theta \approx \hbar$. Convergence (and divergence) of trajectories in a classically chaotic system is governed by the Lyapunov instability exponent λ as, e.g., $\delta \theta(t) \sim \exp\{-\lambda t\}$. It thus takes time $t_E \sim \lambda^{-1} \ln(1/\hbar)$ before the interference effects can reveal themselves.

As we show below, for $K \gg 1$ the quantitative definition of the Ehrenfest time for the QKR is given by

$$t_E = \frac{1}{\lambda} \ln \sqrt{\frac{K}{\hbar}}, \quad (2)$$

while the classical Lyapunov exponent is $\lambda = \ln(K/2)$.⁹ Therefore, there is the parametric regime $1 \ll K \ll \hbar^{-1}$, or more precisely

$$\ln\left(\frac{1}{\hbar}\right) \gg \ln K > 0, \quad (3)$$

where there exists a wide separation of the relevant time scales

$$1 \ll t_E \ll t_L. \quad (4)$$

One may expect that such regime is amenable for an *analytical* treatment of the classical-to-quantum crossover. This problem was first tackled by Aleiner and Larkin²⁷ in the context of random classical (long-range) potential scattering (e.g., random Lorentz gases). However, due to the complexity of the Lorentz gas classical dynamics, their treatment required a regularization. The latter is essentially a weak quantum scattering potential added to the Lorentz gas.

The purpose of this paper is to develop a systematic first-principles analytic treatment of the QKR. In particular, we are able to incorporate the semiclassical dynamics at the scale of t_E into the weak dynamical localization theory without introducing any regularization. The QKR thus allows one to demonstrate explicitly an essential point: *existence of the dynamical localization is an intrinsic property of quantized classically chaotic systems—not an artifact of an extraneous regularization.* (Remarkably, the Ehrenfest time does *not* depend on the regularizer strength.)^{28–30} This observation is fully consistent with the early studies of Ehrenfest time,^{21,22} which suggested the existence of such time scale. For the time interval $t \lesssim t_L$, our approach fully encompasses the Ehrenfest regime. The results were reported in Ref. 29. The

main result for the time-dependent spread of the wave packet may be formulated as

$$\delta \langle l^2(t) \rangle = 2D_{cl} \left[t - \frac{4}{3\sqrt{\pi}} \theta(t - 4t_E) \frac{(t - 4t_E)^{3/2}}{t_L^{1/2}} \right], \quad (5)$$

where $\theta(t)$ is the standard Heaviside step function. The first term describes the classical diffusion, which is the main subject of Sec. III B. The second term is the essential result of the present work and will be derived in Sec. IV B 3. At intermediate times, $t_E \ll t < t_L$, Eq. (5) crosses over to the standard weak-localization correction.¹⁸ At shorter times, $t \approx t_E$, there is a delay in developing localization given by $4t_E$. A few comments are in order: (i) the actual delay is not absolutely sharp, as suggested by Eq. (5). There are exponentially small deviations from the straight line $2D_{cl}t$ even for $t < 4t_E$, the exact shape of which is calculated below. (ii) Equation (5) describes quantum correction *linear* in \hbar that appears to be delayed by $4t_E$. As first noticed by Shepelansky,³¹ *quadratic* in \hbar corrections show up at even earlier time. However, for at least the first three kicks, they may be fully absorbed into a renormalization of the diffusion constant³¹ ($\delta D_{cl} \sim \hbar^2$, essentially due to the change in the scattering cross section). It is thus an oversimplification to claim the absence of quantum effects at $t < 4t_E$. (iii) Equation (5) constitutes the one-loop weak-localization correction. Below, we report also the results of the two-loop calculation. It brings the next-order correction $\sim \theta(t - 2mt_E)(t - 2mt_E)^2/t_L$, $m=3,4$, which also “protects” the early time evolution from the localization effects. It is still an open problem to sum up the entire series to develop a theory of strong localization that accounts for the Ehrenfest time phenomena.

Most of the existing experiments on atomic gases^{3,32,33} do not fall into the parametric regime (3), but rather have $\hbar \approx 1$. In this case $t_E \approx 1$ and our result, Eq. (5), can only be viewed as a qualitative one. We discuss below other possible realizations of the QKR that utilize driven Josephson junctions.^{34,35} Such systems may prove to be more suitable for exploring the parametric regime (3) and thus for a quantitative comparison with the theory.

The outline of the rest of this paper is as follows: Sec. II is devoted to a qualitative semiclassical picture of the weak-dynamical localizations and the Lyapunov regime. Sections III–V serve to quantify these ideas. In Sec. III the diffusion in the phase space of the kicked rotor is obtained as a classical approximation to the full quantum propagation. Section IV is the central part of the present work. It formulates a general framework to deal with the weak-dynamical localization at the semiclassical level. In particular, we calculate the frequency-dependent one-loop correction to the classical diffusion coefficient, and study its effect on the momentum dispersion. This formalism is applied in Sec. V to a modified QKR with broken time-reversal symmetry. The frequency-dependent quantum corrections are calculated at the two-loop level. Experimental realizations of some driven quantum systems are discussed in Sec. VI. The effects of noise

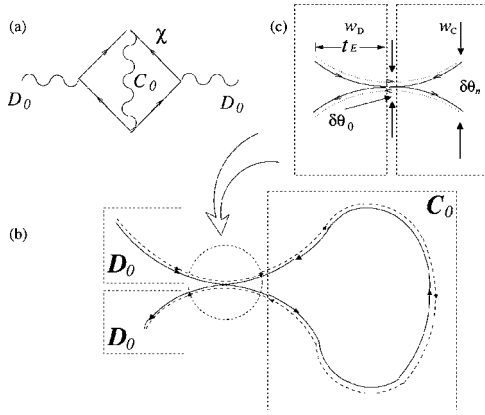


FIG. 1. The first quantum correction to the density-density correlator: (a) one-loop weak localization diagram; (b) trajectory in the momentum space; (c) Hikami box along with Lyapunov portions of the cooperon and diffusons.

and dephasing are the subject of Sec. VII. We conclude in Sec. VIII. Some technical details are delegated the Appendixes.

II. QUALITATIVE CONSIDERATIONS

The physics of the weak-localization corrections is traditionally discussed in the language of classical trajectories. The classical motion of a particle in the random potential is characterized by a rapid randomization of momenta and diffusion spreading of the coordinate. It is thus customary to visualize a trajectory in the coordinate space as a random motion between static impurities. It is straightforward to develop a similar approach for the QKR. In the kicked rotor problem the roles of coordinate and (angular) momentum are interchanged. Indeed, for $K \gg 1$ the angular coordinate θ is rapidly randomized (over the interval $[-\pi, \pi]$), while the angular momentum l acquires a (quasi) random change $\in [-K, K]$. The latter results in the diffusion in the space of angular momentum (see below). We shall thus visualize a “trajectory” as a sequence of values of the angular momentum that kicked rotor “visits” upon successive kicks, Fig. 1(b).

For a quantitative description of the classical motion, it is convenient to monitor pairs of angle and angular momentum in discrete moments of time. This maps the classical dynamics onto a so-called standard map

$$\begin{aligned} l_{n+1} &= l_n + K \sin \theta_n, \\ \theta_{n+1} &= \theta_n + l_{n+1}. \end{aligned} \quad (6)$$

Notice that l_n stands for the angular momentum immediately after the $(n-1)$ -th kick, and θ_n for the angle before the n th kick. It is now obvious that the two successive points of the trajectory, l_n and l_{n+1} , differ by $K \sin \theta_n$. As a first approximation one may treat θ_n as uniformly distributed over $[0, 2\pi]$ and thus $\langle (l_{n+1} - l_n)^2 \rangle = K^2 \langle \sin^2 \theta \rangle = K^2/2$. As a result, $\langle (l_n - l_0)^2 \rangle = 2D_{cl}n$ with $D_{cl} = K^2/4$. An account of the residual correlations between successive θ_n 's, leads to a renormaliza-

tion of D_{cl} with the next term scaling as $K^{3/2}$, etc.^{10,11} For completeness of the presentation we shall derive the full result for the classical diffusion constant in Appendix A. For the current qualitative discussion it is enough to appreciate that a trajectory of the classical kicked rotor exhibits random hops in the space of angular momentum, leading to

$$\delta \langle l^2(t) \rangle \sim 2D_{cl}t. \quad (7)$$

This result has a simple physical interpretation: the average energy of the kicked rotor linearly increases with time, reflecting a constant rate Joel's heating. It is exactly this property of the classical kicked rotor that made it useful in accelerator physics.^{9,10}

In the quantum problem an *amplitude* to evolve from an initial to a finite point in the angular momentum space is given by the sum of *amplitudes* of all classically allowed trajectories passing through these two points. Generically, different trajectories come with random and uncorrelated phases and thus do not produce a systematic interference contribution. An exception to this rule comes from the trajectories having almost (up to \hbar) exactly the same geometrical length and thus the same phase. This situation takes place if a trajectory contains a self-intersection point in the angular momentum space. Then, another trajectory may exist that is identical to the initial one safe for the direction of propagation along the loop; see Fig. 1(b). The fact that the backward propagation along the loop is consistent with the equations of motion is guaranteed by the time-reversal symmetry of the Hamiltonian

$$l \rightarrow l, \quad \theta \rightarrow -\theta, \quad t \rightarrow -t, \quad H \rightarrow H. \quad (8)$$

(Compare it with the time-reversal symmetry in the random potential problem: $\mathbf{r} \rightarrow \mathbf{r}, \mathbf{p} \rightarrow -\mathbf{p}, t \rightarrow -t$.) It is thus easy to see that we are interested in the loops that not only have (almost) coinciding initial and finite momenta: $l_1 \approx l_0$, but also (almost) opposite initial and finite angles: $\theta_1 \approx -\theta_0$. The allowed uncertainty is limited by the effective Planck constant: $(l_1 - l_0)(\theta_1 + \theta_0) \lesssim \hbar$.

Since such two trajectories have (almost) the same phase, they interfere constructively and thus lead to a systematic (localization) quantum correction. The probability to complete the loop in time t is called cooperon and denoted as $\mathcal{C}(l_0, \theta_0; l_1, \theta_1; t)$. With the above-mentioned conditions on the initial and finite points, one may estimate it as $\mathcal{C}(t) \sim \sqrt{D_{cl}/t}$ (this must be multiplied by \hbar to take into account the phase area of the allowed uncertainty). This estimate translates (basically by the double integration over time) to the $-\hbar \sqrt{D_{cl}t^{3/2}}$ correction^{1,18} to the classical law: $\delta \langle l^2(t) \rangle = 2D_{cl}t$. At $t \sim t_L = D_{cl}/\hbar^2$ the correction exceeds the classical result and the QKR crosses over to the strong localization regime.

The qualitative reasoning given above is identical to the one employed in the discussion of a particle in the field of the “quantum” white-noise random potential. However, the kicked rotor dynamics possesses a very important distinction from that of the white-noise potential problem. The latter is the process without a memory. Indeed, two classical trajec-

tories that identically retrace each other up to a certain point may take completely different roots (in particular, counter-propagating ones) after a *single* “quantum” scattering event. After completing the loop in the opposite directions according to the classical random walk dynamics, another *single* quantum scattering makes the two trajectories identical again. These two (actually four, since there are two trajectories involved) quantum scattering events constitute the so-called, Hikami box,³⁶ denoted by \mathcal{X} in Fig. 1(a).

Contrary to this scenario, the kicked rotor scattering events are purely classical, namely the free rotation of the angle. Indeed the trajectory is uniquely defined by the standard map, Eq. (6), sequence. If two trajectories coincide *exactly* at some point (θ_n, l_n) , they continue to be identical [determined by Eq. (6)] forever. This seemingly precludes any possibility to develop the weak-localization scenario outlined above. The way out of this apparent paradox is to recall that the loop may be completed not exactly, but rather up to a small uncertainty: $\delta l \delta \theta \lesssim \hbar$. This small initial difference is magnified (more precisely, exponentially increases) upon successive kicking (Lyapunov instability), leading eventually to the two counterpropagating diffusive roots. The situation is rather similar to the localization in the field of the *classical* large-scale random potential (so-called random Lorentz gas). The latter was considered by Aliener and Larkin some time ago.²⁷ Due to the complexity of the Lorentz gas dynamics, they had to introduce quantum impurities (essentially a weak white-noise component of the scattering potential) to treat the problem analytically. The beauty of the QKR is in the simplicity of its classical dynamics, Eq. (6), that allows one to treat the Lyapunov regime exactly without involving an artificial quantum scattering.

To proceed in this direction, consider two trajectories that initially happen to be at a small distance from each other in the phase space: $(\delta\theta, \delta l)$. Taking variation of Eq. (6), we find that the angle difference evolves as $\delta\theta_n = \delta\theta_{n-1}(1 + K \cos \theta_{n-1}) + \delta l_{n-1}$. In the limit $K \gg 1$ it leads to $\delta\theta_n = (\delta\theta + \delta l/K) \prod_{k=0}^{n-1} (1 + K \cos \theta_k) \approx (\delta\theta + \delta l/K) e^{\lambda n}$, where λ is the Lyapunov exponent. For $K \gg 1$ one finds $\lambda = \langle \ln(K \cos \theta) \rangle = \ln(K/2)$,^{9,10} with the residual term $\sim O(1/K)$. For $\delta\theta \delta l \approx \hbar$, the optimal value of $(\delta\theta + \delta l/K)$ is $\sqrt{\hbar/K}$. It thus takes time $n = t_E = \lambda^{-1} \ln \sqrt{K/\hbar}$, cf. Eq. (2), to evolve from the initial angular uncertainty $\delta\theta \approx \sqrt{\hbar/K} \ll 1$ up to $\delta\theta_n \approx 1$, when the diffusive motion takes over. Once this deviation is reached, the usual diffusive spread of the two trajectories takes place. The time-reversal invariance dictates that the aforementioned divergence of the two trajectories is preceded by their convergence. The latter takes another t_E kicks to be completed. The total duration of the one-way travel through the Lyapunov region is thus $2t_E$. The entire weak-localization loop construction requires two such travels (each including convergence and divergence) through the Lyapunov regime. As a result, the localization corrections are delayed by (cannot be developed in time less than) $4t_E$; see Eq. (5).

Technically there are two equivalent ways to incorporate the Lyapunov region into the weak-localization calculations; see Fig. 1(c). One approach, adopted in Ref. 27, is to redef-

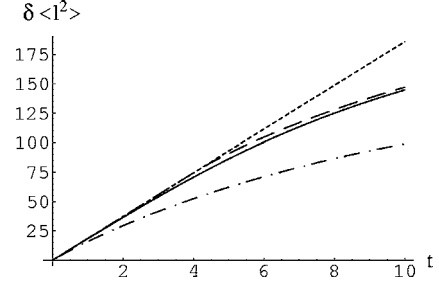


FIG. 2. The momentum dispersion for $K=6.1$ and $\hbar=0.6$ ($4t_E=4.2$)—full line; the classical limit ($\hbar \rightarrow 0$)—dashed line; standard weak localization ($t_E=0$)—dashed-dotted line; the limit $\lambda_2 \rightarrow 0$, Eq. (5)—long-dashed line.

fine the Hikami box to contain $4t_E$ scattering events (kicks) instead of the conventional four. Then, cooperon (and the diffusons) is just a conventional diffusive propagator in the momentum space. In the present paper we find it convenient to follow the traditional treatment of the Hikami box as consisting of the four kicks. These four kicks are treated exactly by multiplying the corresponding quantum evolution operators. It is the analytical expression for the Hikami box that dictates allowed deviations of the $\delta l \delta \theta$ product. The Lyapunov regimes are delegated to the “legs” of the cooperon (and diffusons). The latter is now understood as a propagator that includes both Lyapunov-type divergence-convergence of the close trajectories along with the normal diffusion once a macroscopic deviation between them is reached. As we show below, the choice of the four kicks in the Lyapunov regime, coined to be the Hikami box is immaterial. For any such choice the quantum correction, linear in \hbar , is delayed by $4t_E$. It is important to mention that the time interval $0 < t < 4t_E$ is protected from the higher-order loop corrections as well. To demonstrate this fact we performed the two-loop weak-localization calculation, and found that the corresponding contribution consists of two parts: $\delta \langle l^2 \rangle \sim D_{cl} \theta (t - 2mt_E)(t - 2mt_E)^2 / t_L$, $m=3, 4$, which are delayed by $6t_E$ and $8t_E$, respectively.

The delay is not absolutely sharp, but rather is slightly smeared by $\delta t_E \equiv \sqrt{\lambda_2 t_E / \lambda^2} \ll t_E$ number of kicks. The reason for this smearing is in fluctuations of the exponent λ . Such fluctuations are due to the fact that one follows the Lyapunov instability for a finite number of kicks only. (Indeed, unlike classical problems, the minimal deviation is limited by \hbar and thus the time to leave the Lyapunov regime is finite and may fluctuate between the trajectories.) Following Ref. 27, we characterize fluctuations of the Lyapunov exponent by the other exponent, λ_2 (for QKR with $K \gg 1$ one finds $\lambda_2 \approx 0.82$). In the case $t_E \gg 1$, cf. Eq. (3), the effect of smearing due to λ_2 is rather small.

The predicted time-dependent momentum dispersion graph is plotted in Fig. 2. The following sections serve to quantify the qualitative semiclassical picture outlined above.

III. CLASSICAL LIMIT: DIFFUSON AND COOPERON

We proceed now to develop the qualitative considerations outlined above into an accurate theory of the QKR. The es-

sential starting point is the classical diffusion in the angular momentum direction of the classical phase space: $[-\pi, +\pi] \times [-\infty, +\infty]$. We will clarify first how to find the classical diffusion from the exact quantum correlator. One starts by introducing the exact one period quantum evolution operator as

$$\hat{U} \equiv \hat{V}\hat{J},$$

$$\hat{V} = \exp(i\hat{l}^2/2\kappa), \quad \hat{J} = \exp(iK \cos \hat{\theta}/\kappa). \quad (9)$$

All physical quantities may be expressed in terms of the matrix elements of \hat{U}^n , where n stands for the number of kicks (time). We are particularly interested in the four-point “density-density” correlator, defined as

$$\mathcal{D}(l_+, l_-; l'_+, l'_-; n, n') \equiv \langle l_+ | \hat{U}^n e^{i\hat{l}^2/2\kappa} | l'_+ \rangle \langle l_- | \hat{U}^{n'} e^{i\hat{l}^2/2\kappa} | l'_- \rangle^*, \quad (10)$$

where $|l_\pm\rangle$ denotes the basis of discrete momentum eigenstates of $K=0$ quantum Hamiltonian. Note that the forward and backward trajectories in this expression are, in general, different. However, it is natural to expect, after some transient processes, the correlator will be dominated by the case of $n=n'$. This is easy to see by Fourier transforming the correlator with respect to n, n' , passing to the frequency (ω_+, ω_-) representation

$$\mathcal{D}(l_+, l_-; l'_+, l'_-; \omega_+, \omega_-) = \sum_{n, n'=0} e^{i(\omega_+ n - \omega_- n')} \mathcal{D}(l_+, l_-; l'_+, l'_-; n, n') \quad (11)$$

and subsequent averaging over $(\omega_+ + \omega_-)/2$. Let us denote such correlator thereby obtained as $\mathcal{D}(l_+, l_-; l'_+, l'_-; \omega)$, where $\omega = \omega_+ - \omega_-$. From Eq. (10) one may check that it satisfies

$$\begin{aligned} \mathcal{D}(l_+, l_-; l'_+, l'_-; \omega) &= e^{[i(l_+^2 - l_-^2)]/2\kappa} \delta_{l_+, l'_+} \delta_{l_-, l'_-} + e^{i\omega} \sum_{l''_+, l''_-} \langle l_+ | \hat{U} | l''_+ \rangle \\ &\times \langle l_- | \hat{U} | l''_- \rangle^* \mathcal{D}(l''_+, l''_-; l'_+, l'_-; \omega). \end{aligned} \quad (12)$$

The matrix elements $\langle l_+ | \hat{U} | l''_+ \rangle$ and $\langle l_- | \hat{U} | l''_- \rangle^*$ may be explicitly written as

$$\begin{aligned} \langle l_+ | \hat{U} | l''_+ \rangle \langle l_- | \hat{U} | l''_- \rangle^* &= \int \int \frac{d\theta_+ d\theta_-}{2\pi 2\pi} \exp \left[\frac{il_+^2}{2\kappa} + \frac{iK \cos \theta_+}{\kappa} \right. \\ &+ \left. \frac{i\theta_+}{\kappa} (l_+ - l''_+) \right] \exp \left[-\frac{il_-^2}{2\kappa} - \frac{iK \cos \theta_-}{\kappa} \right. \\ &- \left. \frac{i\theta_-}{\kappa} (l_- - l''_-) \right]. \end{aligned} \quad (13)$$

For what follows, it is convenient to introduce the Wigner transform representation as

$$\begin{aligned} \mathcal{D}(l, \theta; l', \theta'; \omega) &\equiv \sum_{l_+, l_-} \sum_{l'_+, l'_-} \exp \left(-\frac{i}{\kappa} [(l_+ - l_-)\theta \right. \\ &- \left. (l'_+ - l'_-)\theta'] \right) \mathcal{D}(l_+, l_-; l'_+, l'_-; \omega), \end{aligned} \quad (14)$$

where we define $l \equiv (l_+ + l_-)/2$ and $l' \equiv (l'_+ + l'_-)/2$.

A. Frobenius-Perron-Ruelle equation: Classical kicked rotor

Let us consider a solution of Eq. (12). As we will see below, the integral over θ_\pm in Eq. (13) is dominated by $|\theta_+ - \theta_-| \sim \kappa/K \ll 1$. This then allows for a perturbative expansion of $|\theta_+ - \theta_-|$ in the exponent of Eq. (13). In this subsection we show that the leading term in such expansion leads to the classical equation of motion (standard map), Eq. (6) (so-called “semiclassical approximation”). The semiclassical solution thereby obtained is denoted as \mathcal{D}_0 . It should be emphasized that the classical diffusive propagator cannot be recovered at this stage. To achieve this goal, the further approximation must be used, which will be clarified in Sec. III B.

The semiclassical treatment employs the following approximation for $\langle l_+ | \hat{U} | l''_+ \rangle \langle l_- | \hat{U} | l''_- \rangle^*$ matrix elements:

$$\begin{aligned} \cos \theta_+ - \cos \theta_- &= -2 \sin \frac{\theta_+ - \theta_-}{2} \sin \frac{\theta_+ + \theta_-}{2} \\ &\approx -(\theta_+ - \theta_-) \sin \frac{\theta_+ + \theta_-}{2} \end{aligned} \quad (15)$$

in the limit $|\theta_+ - \theta_-| \ll 1$. With this approximation, Eq. (13) is simplified as

$$\begin{aligned} \langle l_+ | \hat{U} | l''_+ \rangle \langle l_- | \hat{U} | l''_- \rangle^* &\approx \int \int \frac{d\theta_+ d\theta_-}{2\pi 2\pi} \exp \left[\frac{i(l_+ + l_-)(l_+ - l_-)}{2\kappa} \right. \\ &- \left. \frac{iK}{\kappa} \sin \frac{\theta_+ + \theta_-}{2} (\theta_+ - \theta_-) \right] \\ &\times \exp \left\{ \frac{i}{\kappa} (\theta_+ - \theta_-) \left(\frac{l_+ + l_-}{2} - \frac{l''_+ + l''_-}{2} \right) \right. \\ &+ \left. \frac{i}{\kappa} \frac{\theta_+ + \theta_-}{2} [(l_+ - l_-) - (l''_+ - l''_-)] \right\}. \end{aligned} \quad (16)$$

Let us insert it into Eq. (12) and perform the Wigner transform. We also define $\theta \equiv (\theta_+ + \theta_-)/2$ and $\theta' \equiv (\theta'_+ + \theta'_-)/2$ to simplify the notations. Then, with $(\theta_+ - \theta_-)/\kappa$, $(l_+ - l_-)/\kappa$, $(l'_+ - l'_-)/\kappa$, and $(l''_+ - l''_-)/\kappa$ integrated out, we obtain

$$\begin{aligned} \mathcal{D}_0(l, \theta; l', \theta'; \omega) &= 2\pi\kappa \delta(l - l') \delta(\theta - \theta' - l) \\ &+ e^{i\omega \vec{P}} \mathcal{D}_0(l, \theta; l', \theta'; \omega), \end{aligned} \quad (17)$$

where \vec{P} is the Frobenius-Perron-Ruelle (FPR) operator, acting on the nearest two arguments from the left according to

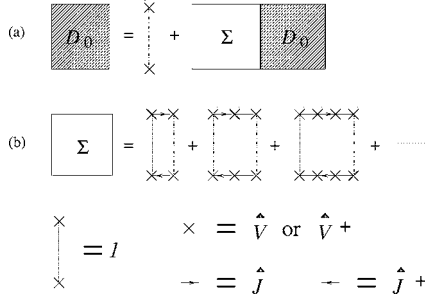


FIG. 3. Schematic representation for the diffusion approximation of classical density-density correlator—the solution of Frobenius-Perron-Ruelle equation (a), with the self-energy (b). The structure of the self-energy is such that the beginning and ending (after τ_c kicks) pairs of the angular momenta are the same (denoted by vertical dot-dashed line), while the other pairs are not.

$$\begin{aligned} \vec{P}f(l, \theta; l', \theta') &\equiv \int \int dl_1 d\theta_1 \delta(l - l_1 - K \sin \theta_1) \delta(\theta - \theta_1 - l) \\ &\times f(l_1, \theta_1; l', \theta'), \end{aligned} \quad (18)$$

where $f(l, \theta; l', \theta')$ is an arbitrary function. The kernel above implies that the correlator thereby obtained describes the deterministic motion of *classical* kicked rotor, i.e., standard mapping. Note that, in the time representation, \mathcal{D}_0 is normalized, namely $(2\pi\hbar)^{-1} \int \int dl d\theta \mathcal{D}_0(l, \theta; l', \theta'; n) = 1$.

B. Diffusion approximation

To recover the classical diffusion, the procedure of deriving the FPR equation must be appropriately regularized.^{11,12,37} Indeed, in the presence of noises one is able to do so and find the proper diffusion constant. We shall not follow this procedure here, but rather refer the reader to Refs. 11 and 12.

We shall show below, however, that a regularization is consistent with the generalization of Altland's¹⁸ diagrammatic method. The latter starts from the exact quantum density-density correlator, Eq. (10), and leads to the classical diffusion with the correct diffusion constant. The basic idea is that the *normal* diffusion implies the existence of some time scale, τ_c , and results from the evolution (determined by the standard mapping) taking place at this time scale. In other words, τ_c is the longest time the memory about initial conditions of a generic classical trajectory is kept. For example, in the case of $\tau_c=1$ (see below), only the one-step process contributes to the diffusion constant, which in fact occurs at the limit $K \rightarrow \infty$. For smaller K , τ_c becomes longer (for example, say $\tau_c=2$; see Appendix A for a detailed discussion). In such a case, the diffusion constant is contributed by the one-step and two-step process. Technically, complementing the semiclassical approximation: $|\theta_{n_+} - \theta_{n_-}| \ll 1$, $n = 1, 2, \dots$, it is further required that $l_+ = l_- \equiv l$ and $l'_+ = l'_- \equiv l'$ at two ends, as well as $l''_+ = l''_- \equiv l''$ for the intermediate variables at multiple times of τ_c .

For $\tau_c=1$ the angular memory is lost after every kick [cf. the first diagram on the right-hand side of Fig. 3(b)]. In this approximation Eq. (12) is reduced to

$$\mathcal{D}_0(l, l'; \omega) = \delta_{l, l'} + e^{i\omega} \sum_{l''} \langle l | \hat{U} | l'' \rangle \langle l | \hat{U} | l'' \rangle^* \mathcal{D}_0(l'', l'; \omega), \quad (19)$$

where the matrix element $\langle l | \hat{U} | l'' \rangle \langle l | \hat{U} | l'' \rangle^*$ is explicitly written as

$$\begin{aligned} \langle l | \hat{U} | l'' \rangle \langle l | \hat{U} | l'' \rangle^* &= \langle l | \hat{J} | l'' \rangle \langle l | \hat{J} | l'' \rangle^* \\ &= \int \int \frac{d\theta_+ d\theta_-}{2\pi} \exp \left[\frac{iK}{\hbar} (\cos \theta_+ - \cos \theta_-) \right] \\ &\times \exp \left[\frac{i(\theta_+ - \theta_-)(l - l'')}{\hbar} \right] \\ &= \int \int \frac{d\theta_+ d\theta_-}{2\pi} \exp \left[-\frac{2iK}{\hbar} \right. \\ &\times \sin \frac{\theta_+ + \theta_-}{2} \sin \frac{\theta_+ - \theta_-}{2} \left. \right] \\ &\times \exp \left[\frac{i(\theta_+ - \theta_-)(l - l'')}{\hbar} \right]. \end{aligned} \quad (20)$$

From this we see (as mentioned above) that the integral is dominated by $|\theta_+ - \theta_-| \sim \hbar/K$. Making the change of variables: $(\theta_+, \theta_-) \rightarrow [(\theta_+ + \theta_-)/2, \theta_+ - \theta_- \equiv \hbar\varphi]$ and integrating out $(\theta_+ + \theta_-)/2$, we simplify Eq. (20) as¹⁸

$$\langle l | \hat{U} | l'' \rangle \langle l | \hat{U} | l'' \rangle^* \approx \int \frac{d\varphi}{2\pi} J_0 \left[\frac{2K}{\hbar} \sin \frac{\hbar\varphi}{2} \right] e^{i\varphi(l - l'')}. \quad (21)$$

Here, $J_n(x)$ is the Bessel function of order n . Turning to the Fourier representation: $\mathcal{D}_0(\varphi; \omega) \equiv \sum_{l, l'} e^{-i\varphi(l - l')} \mathcal{D}_0(l - l'; \omega)$, Eq. (19) gives the classical propagator as

$$\mathcal{D}_0(\varphi; \omega) = \frac{1}{1 - e^{i\omega} J_0 \left[\frac{2K}{\hbar} \sin \frac{\hbar\varphi}{2} \right]}. \quad (22)$$

In the limit $\omega \ll 1$, $K\varphi \ll 1$, it is reduced to the usual diffuson (Fig. 3)

$$\mathcal{D}_0(\varphi; \omega) \approx \frac{1}{-i\omega + D_{cl}\varphi^2}, \quad (23)$$

with the diffusion constant $D_{cl}(K) = K^2/4$.

In Ref. 11, it was shown that the higher-order correlations, namely $\tau_c > 1$ [e.g., the second, third, etc. diagrams on the right-hand side of Fig. 3(b)] lead to the modification of the diffusion constant according to

$$D_{cl}(K) = \frac{K^2}{4} [1 - 2J_2(K) - 2J_1^2(K) + 2J_2^2(K) + \dots]. \quad (24)$$

It is worth pointing out that, although the original derivation is based on pure classical considerations, it is fully compatible with the general formalism developed in this paper. For clarification, we reproduce Eq. (24) from the exact quantum

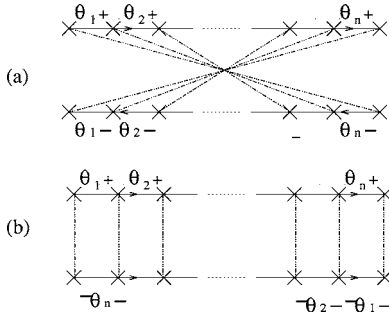


FIG. 4. The diffusive cooperon approximation for the classical density-density correlator. Typical diagrammatic representation for the classical cooperon ($|\theta_{1+} + \theta_{n-}|, |\theta_{2+} + \theta_{(n-1)-}|, \dots \ll 1$) (a). Rotating the bottom line of (a) retrieves classical diffuson with θ_{k-} replaced by $-\theta_{k-}$ ($k=1, 2, \dots, n$) (b).

density-density correlator, Eq. (12), in Appendix A. We emphasize that throughout the paper all the higher-order terms in Eq. (24) may be reproduced wherever the classical constant D_{cl} is involved. However, for sufficiently large K , which is of interest in the present work, these corrections are unimportant and thereby neglected.

In the long time limit, the validity of a diffusion description for the classical dynamics is affected by two factors, namely values of K and initial data in the phase space. It is believed that in general, for sufficiently large K there exist stable islands in the phase space, starting from which a trajectory exhibits quasiperiodic motion.^{9,10} It has been estimated, however, that the total area of these islands on the phase space is exponentially small in the limit $K \gg 1$.^{9,23} Our approximation, being an expansion in powers of $1/K$, is bound to lose information about these islands. It is also known (see, e.g., Ref. 12) that even a trajectory starting from the chaotic region may stick to these islands beyond some *classical* time scale. However, for most values of $K (\gg 1)$ this time scale is extremely large and thereby opens a large region where *classical* normal diffusion takes place. On the other hand, for some parametric regions of K , there appear some peculiar islands (so-called “accelerator mode”^{9,10}), starting from or near which a trajectory will be boosted, faster than the normal diffusion.³⁸ (Similar phenomena exist also in a generic model.^{10,32}) To conclude, throughout the paper we will focus on sufficiently large K and stay away from those parametric regions exhibiting the accelerator modes. It thereby becomes a reasonable assumption that the sticking time is much longer than any other time scales that are relevant for the present work.

C. Classical cooperon

Starting from the exact quantum density-density correlator, one may see that the classical diffuson is defined diagrammatically as the sum over all diagrams such as $|\theta_{1+} - \theta_{1-}| \sim |\theta_{2+} - \theta_{2-}| \cdots \sim |\theta_{n+} - \theta_{n-}| \ll 1$. In this part, we turn to the discussion of another family of diagrams defining the cooperon. To this end we focus on the sum over all the diagrams such as $|\theta_{1+} + \theta_{n-}| \sim |\theta_{2+} + \theta_{(n-1)-}| \cdots \sim |\theta_{n+} + \theta_{1-}| \ll 1$ (cf. Fig. 4 for notations). Notice that the cooperon essentially

is a classical object since it becomes identical to the diffuson under the TRS operation: $\theta_{k+} \rightarrow \theta'_{k+} = \theta_{k+}$ and $\theta_{k-} \rightarrow \theta'_{k-} = -\theta_{(n+1-k)-}$.

1. Diffusion approximation of the solution of FPR equation

To find the density-density correlator in this limit, let us turn to the Wigner representation [notice the crucial difference from Eq. (14)]

$$\begin{aligned} \mathcal{C}(l, \theta; l', \theta'; \omega) \equiv & \sum_{l_+ - l'_+} \sum_{l'_+ - l_-} \exp\left(-\frac{i}{\hbar}[(l_+ - l'_+) \theta - (l'_+ - l_-) \theta']\right) \\ & \times \mathcal{C}(l_+, l_-; l'_+, l'_-; \omega), \end{aligned} \quad (25)$$

where we define $l \equiv (l_+ + l'_+)/2$ and $l' \equiv (l'_+ + l_-)/2$. The key observation is that the diffuson diagram may be retrieved with the bottom (advanced Green function) line [Fig. 4(a)] rotated. This is due to the fact that such a procedure simply leads to the time reversal of the series: $\theta_{1-} \rightarrow \theta_{2-} \rightarrow \cdots \rightarrow \theta_{n-}$ such that it becomes $-\theta_{n-} \rightarrow -\theta_{(n-1)-} \rightarrow \cdots \rightarrow -\theta_{1-}$. For this reason, we call it cooperon, as introduced in Sec. II. Since $|\theta_{1+} + \theta_{n-}| \ll 1$, we may proceed along the lines of derivation of Eq. (17) from Eqs. (12) and (14), and arrive at

$$\begin{aligned} \mathcal{C}_0(l, \theta; l', \theta'; \omega) = & 2\pi\hbar\delta(l - l')\delta(\theta - \theta' - l) \\ & + e^{i\omega} \vec{P} \mathcal{C}_0(l, \theta; l', \theta'; \omega). \end{aligned} \quad (26)$$

That is, the classical cooperon is also a solution of the FPR equation.

The only difference with the diffuson is that, instead of having poles at $\hbar\varphi \equiv \theta_+ - \theta_-$, the Cooperon has poles at $\hbar\varphi \equiv \theta_+ + \theta_-$ (i.e., $\hbar\varphi \equiv \theta_{1+} + \theta_{n-} = \theta_{2+} + \theta_{(n-1)-} = \cdots = \theta_{n+} + \theta_{1-}$). One concludes, thus, that the diffusive form, Eq. (23), holds in the limit $\omega \ll 1, K\varphi \ll 1$ (cf. Fig. 4) for the cooperon as well. In particular, in the case of $|\theta + \theta'| \sim 1$, the averaging over $(\theta + \theta')/2$ may be performed. Furthermore, if $|l - l'| \leq K$, then \mathcal{C}_0 does not depend on the angular momenta. In other words

$$\begin{aligned} \mathcal{C}_0(l, \theta; l', -\theta'; \omega) & = \langle \mathcal{C}_0(l, \theta; l', -\theta'; \omega) \rangle_{(\theta + \theta')/2} \\ & = \int \frac{d\varphi}{2\pi} \frac{\hbar}{-i\omega + D_{cl}\varphi^2} \equiv \langle \mathcal{C}_0(\omega) \rangle, \end{aligned} \quad (27)$$

where $|l - l'| \leq K$, and $|\theta - \theta'| \sim 1$.

2. Treatment of the Lyapunov instability regime

The above general solution for the classical cooperon, $\mathcal{C}_0(l, \theta; l', -\theta'; n)$, characterizes the probability for a trajectory, initiating from (l, θ) , to end at $(l', -\theta')$. From now on we focus on a special case, where $\delta l_0 \equiv l - l'$; $\delta\theta_0 \equiv \theta - \theta'$ are small such that $|\delta l_0| \leq K, |\delta\theta_0| \leq 1$. In this part we show that it differs from $\langle \mathcal{C}_0(\omega) \rangle$ by a renormalization factor.

Without loss of generality, we assume that $\mathcal{C}_0(l, \theta; l', -\theta'; n)$ evolves from some initial distribution $f(l, \theta; l', -\theta')$, bearing the symmetry of $f(l, \theta; l', -\theta') = f(l', \theta'; l, -\theta)$. Then,

the formal solution of the FPR equation is given by

$$C_0(l, \theta; l', -\theta'; n) = \tilde{P}^n f(l, \theta; l', -\theta'). \quad (28)$$

To simplify the notations, we rewrite the action of the FPR operator on C_0 as

$$\tilde{P}C_0(l, \theta; l', \theta') = C_0(S^{-1}[l, \theta]; l', \theta'), \quad (29)$$

where S and S^{-1} are defined as

$$\begin{aligned} S[l, \theta] &\equiv (l + K \sin(\theta + l), \theta + l), \\ S^{-1}[l, \theta] &\equiv (l - K \sin(\theta - l), \theta - l), \end{aligned} \quad (30)$$

respectively. Moreover, we introduce the time reversal of the FPR operator, \tilde{P}_T , as

$$\begin{aligned} f(l, \theta; l', \theta') \tilde{P}_T &\equiv \int \int dl_1 d\theta_1 f(l, \theta; l_1, \theta_1) \delta(l_1 - l' \\ &\quad - K \sin \theta_1) \delta(\theta_1 - \theta' - l). \end{aligned} \quad (31)$$

Owing to the symmetry of f , mentioned above, one may introduce the following identity:

$$\tilde{P}f(l, \theta; l', \theta') = f(l, \theta; l', \theta') \tilde{P}_T; \quad (32)$$

its proof is given in Appendix B. Applying this relation repeatedly to the formal solution, Eq. (28), we obtain

$$\begin{aligned} C_0(l, \theta; l', -\theta'; n) &= \tilde{P}^{n-2n'} \{ \tilde{P}^{n'} f(l, \theta; l', -\theta') \tilde{P}_T^{n'} \} \\ &= \tilde{P}^{n-2n'} f(S^{-n'}[l, \theta]; S^{n'}[l', -\theta']), \end{aligned} \quad (33)$$

for an arbitrary integer number n' such that $2n' \leq n$. Consider two nearby trajectories described by (l_1, θ_1) and (l'_1, θ'_1) , respectively. Their motion is induced by $S^{-n}[l, \theta]$ and $S^n[l', -\theta']$, following

$$\begin{aligned} (l_1, \theta_1) &\equiv S^{-n}[l, \theta], \\ (l'_1, -\theta'_1) &\equiv S^n[l', -\theta']. \end{aligned} \quad (34)$$

Associated with the exponential separation of these two nearby trajectories, the time, say n_c , is defined such that

$$|l_{n_c} - l'_{n_c}| \approx K, \quad |\theta_{n_c} - \theta'_{n_c}| \approx 1. \quad (35)$$

At such a moment the separation reaches some macroscopic size. After this time the separation experiences the usual diffusion in the angular momentum space, while the angle difference is uniformly distributed. We substitute then $n' = n_c$ into Eq. (33), and arrive at

$$C_0(l, \theta; l', -\theta'; n) = \theta(n - 2n_c) \langle C_0(n - 2n_c) \rangle, \quad (36)$$

where $\langle C_0(n) \rangle$ is the Fourier transform of $\langle C_0(\omega) \rangle$. Consequently, the Fourier transform of Eq. (33) with respect to n is reduced to

$$C_0(l, \theta; l', -\theta'; \omega) = e^{2i\omega n_c} \int \frac{d\varphi}{2\pi - i\omega + D_{cl}\varphi^2} \bar{\kappa} \quad (37)$$

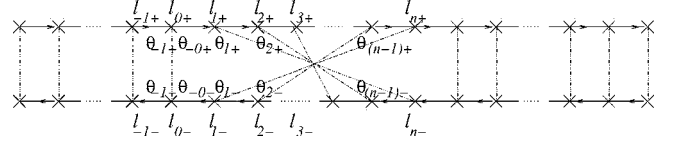


FIG. 5. Sketch of a general diagram, leading to one-loop approximation.

In general, n_c is determined by the initial condition, namely the center of mass: $[(l+l')/2, (\theta+\theta')/2]$ and the initial deviation: $(\delta l, \delta\theta)$. One can perform the change of variables with respect to general separation $(\delta l, \delta\theta)$ according to $z \equiv \ln|\delta\theta|$, $\alpha \equiv \delta l/\delta\theta$. In what follows, z and α are identified as slow and fast variables, correspondingly. If the initial deviation is small enough such that the typical $n_c \gg 1$, the fluctuations of n_c at this time scale are small. As a result, after averaging over initial α , as well as the center of mass, one may cast $\exp[2i\omega n_c]$ into the renormalization factor (with the logarithmic accuracy) as (see Appendix C for details)

$$\mathcal{W}_C(2\omega) \equiv \langle \exp[2i\omega n_c] \rangle = \exp\left(2i\omega t^C - \frac{2\omega^2 \lambda_2 t^C}{\lambda^2}\right), \quad (38)$$

with

$$t^C \equiv \frac{1}{\lambda} \left| \ln \frac{1}{\sqrt{\delta\theta^2 + \delta l^2/K^2}} \right|, \quad (39)$$

in the limit $\omega\lambda_2/\lambda^2 \ll 1$. Consequently, Eq. (37) is reduced to

$$C_0(l, \theta; l', -\theta'; \omega) = \bar{\kappa} \mathcal{W}_C(2\omega) \int \frac{d\varphi}{2\pi - i\omega + D_{cl}\varphi^2}. \quad (40)$$

IV. WEAK-DYNAMICAL LOCALIZATION IN KICKED ROTOR: ONE-LOOP CORRECTION

As explained above, the weak-dynamical localization involves couplings between the diffusons and the cooperon [Fig. 5]. Therefore, one needs a technique to treat two different kinds of the Wigner transforms introduced for diffusons, Eq. (14), and for cooperons, Eq. (25), in a unified way. To develop such a technique is the central task of this section. We show then that the constructive interference between two counterpropagating trajectories leads to the usual one-loop quantum correction, which is a precursor of the dynamical localization. In particular, the one-loop correction to the diffusion constant will be calculated.

A. Exact interaction vertex

We will show in Appendix D 1 that the one-loop correction to the density-density correlator reads as

$$\delta\hat{D} = \hat{D}(e^{i\omega\hat{P}_T} - 1)\hat{C}(e^{i\omega\hat{P}} - 1)\hat{D}, \quad (41)$$

with

$$\hat{C} \equiv e^{i\omega\hat{P}_J}\hat{C}_0e^{i\omega\hat{P}_J}, \quad (42)$$

in the exact quantum operator representation. Here, $\hat{P} \equiv \hat{P}_V\hat{P}_J$ and $\hat{P}_T \equiv \hat{P}_J\hat{P}_V$. The matrix elements of \hat{P}_V and \hat{P}_J are explicitly written as

$$\begin{aligned} \langle l_+, l_- | \hat{P}_V | l'_+, l'_- \rangle &= \exp \left[\frac{i(l_+^2 - l_-^2)}{2\hbar} \right] \delta_{l_+, l'_+} \delta_{l_-, l'_-}, \\ \langle \theta_+, \theta_- | \hat{P}_J | \theta'_+, \theta'_- \rangle &= \exp \left[\frac{iK(\cos \theta_+ - \cos \theta_-)}{\hbar} \right] \\ &\quad \times \delta(\theta_+ - \theta'_+) \delta(\theta_- - \theta'_-), \end{aligned} \quad (43)$$

in the representation of the angular momentum and the angle, correspondingly. Since we are ultimately interested in the long time effects and therefore in the low frequencies, the $e^{i\omega}$ factors in Eqs. (41) and (42) may be safely omitted from now on. Thus, we shall not write them hereafter.

1. Minimal wave packet

In order to calculate $\delta\hat{D}$ explicitly, we consider a general quantity, say $\hat{I}_q \equiv \hat{A}\hat{C}\hat{B}$ [understanding that $\hat{A} = \hat{D}(\hat{P}_T - 1)$, $\hat{B} = (\hat{P} - 1)\hat{D}$ for $\delta\hat{D}$], and write it explicitly as (for simplicity we omit the ω argument)

$$\begin{aligned} \mathcal{I}_q(l_+, l_-; l'_+, l'_-) &= \sum_{l_1, l'_1} \sum_{l_2, l'_2} \sum_{l_3, l'_3} \sum_{l_4, l'_4} \times \mathcal{A}(l_+, l_-; l_1, l'_1) \mathcal{X} \mathcal{C}_0 \\ &\quad \times (l_2, l_3; l'_2, l'_3) \mathcal{B}(l_4, l'_4; l'_+, l'_-), \end{aligned} \quad (44)$$

in the angular momentum representation, where \mathcal{X} is

$$\begin{aligned} \mathcal{X} &= \langle l_1 | e^{i(K/\hbar)\cos \hat{\theta}} | l_2 \rangle \langle l'_1 | e^{i(K/\hbar)\cos \hat{\theta}} | l'_2 \rangle^* \times \langle l_3 | e^{i(K/\hbar)\cos \hat{\theta}} | l_4 \rangle \\ &\quad \times \langle l'_3 | e^{i(K/\hbar)\cos \hat{\theta}} | l'_4 \rangle^*. \end{aligned} \quad (45)$$

Furthermore, we write explicitly the matrix elements of \mathcal{X} , Eq. (45), as

$$\mathcal{X} = \int \int \int \int \frac{d\theta_1}{2\pi} \frac{d\theta'_1}{2\pi} \frac{d\theta_2}{2\pi} \frac{d\theta'_2}{2\pi} \exp \left[\frac{i}{\hbar} (S_{kin} + S_p) \right], \quad (46)$$

where S_{kin} and S_p are defined as

$$S_{kin} = -\theta_1(l_1 - l_2) + \theta'_1(l'_1 - l'_2) - \theta_2(l_3 - l_4) + \theta'_2(l'_3 - l'_4), \quad (47)$$

and

$$S_p = K(\cos \theta_1 - \cos \theta'_1 + \cos \theta_2 - \cos \theta'_2), \quad (48)$$

respectively. For the discussions below, we make the following change of variables:

$$\begin{aligned} \phi &= (\theta_1 - \theta'_1) - (\theta_2 - \theta'_2), \\ \delta l_1 &= \frac{l_2 + l'_3}{2} - \frac{l_3 + l'_2}{2}, \quad \delta \theta_1 = \frac{\theta_1 + \theta'_1}{2} + \frac{\theta_2 + \theta'_2}{2}, \end{aligned}$$

$$\delta l_2 = \frac{l_1 + l'_1}{2} - \frac{l_4 + l'_4}{2},$$

$$\delta \theta_2 = -\frac{1}{2}[(\theta_1 - \theta'_1) + (\theta_2 - \theta'_2)]. \quad (49)$$

Then, S_{kin} may be rewritten as

$$\begin{aligned} S_{kin} &= \frac{\phi}{2} \left[\left(\frac{l_2 + l'_3}{2} + \frac{l_3 + l'_2}{2} \right) - \left(\frac{l_1 + l'_1}{2} + \frac{l_4 + l'_4}{2} \right) \right] + \delta \theta_1 \delta l_1 \\ &\quad + \delta \theta_2 \delta l_2 - \frac{1}{2} \left(\frac{\theta_1 + \theta'_1}{2} - \frac{\theta_2 + \theta'_2}{2} \right) \{ [(l_1 - l'_1) + (l_4 - l'_4)] \\ &\quad - [(l_2 - l'_2) + (l_3 - l'_3)] \} - \frac{\delta \theta_1}{2} [(l_1 - l'_1) - (l_4 - l'_4)] \\ &\quad - \frac{\delta \theta_2}{2} [(l_2 - l'_2) - (l_3 - l'_3)]. \end{aligned} \quad (50)$$

On the other hand, with the semiclassical approximation (i.e., $\theta_{1,2} \approx \theta'_{1,2}$) taken into account, S_p may be written as

$$\begin{aligned} S_p &\approx -2K\delta\theta_2 \sin \left(\frac{\delta\theta_1}{2} \right) \cos \left[\frac{1}{2} \left(\frac{\theta_1 + \theta'_1}{2} - \frac{\theta_2 + \theta'_2}{2} \right) \right] \\ &\quad - K\phi \cos \left[\frac{1}{2} \left(\frac{\theta_1 + \theta'_1}{2} - \frac{\theta_2 + \theta'_2}{2} \right) \right]. \end{aligned} \quad (51)$$

For sufficiently large K , we may average the exponent over the phase $[(\theta_1 + \theta'_1) - (\theta_2 + \theta'_2)]/4$. Moreover, $\delta\theta_{1,2} \approx 0$. Finally, we employ the conventional hydrodynamic approximation, i.e., take into account the leading term in the $K\phi$ expansion only, to arrive at

$$\begin{aligned} \exp \left(\frac{iS_p}{\hbar} \right) &\rightarrow \left\langle \exp \left(\frac{iS_p}{\hbar} \right) \right\rangle \\ &\approx \left\langle \exp \left\{ -\frac{iK\delta\theta_1\delta\theta_2}{\hbar} \right. \right. \\ &\quad \left. \left. \times \cos \left[\frac{1}{2} \left(\frac{\theta_1 + \theta'_1}{2} - \frac{\theta_2 + \theta'_2}{2} \right) \right] \right\} \right\rangle \\ &= J_0 \left(\frac{K\delta\theta_1\delta\theta_2}{\hbar} \right). \end{aligned} \quad (52)$$

Let us insert Eqs. (46), (50), and (52), as well as the Wigner transform of \mathcal{A} , \mathcal{B} [cf. Eq. (14)], and \mathcal{C}_0 [cf. Eq. (25)] into Eq. (44), and integrate out $(l_1 - l'_1)/\hbar$, $(l_4 - l'_4)/\hbar$, $(l_2 - l'_2)/\hbar$, $(l_3 - l'_3)/\hbar$, $(l_+ - l_-)/\hbar$, $(l'_+ - l'_-)/\hbar$, and ϕ/\hbar . As a result, we find that the semiclassical approximation for \mathcal{I}_q is

$$\begin{aligned} \mathcal{I}_q(l, \theta; l', \theta') &= \hat{\mathcal{V}} \left[\mathcal{A}_W \left(l, \theta; l'' + \frac{\delta l_2}{2}, \theta' + \frac{\delta \theta_1}{2} \right) \right. \\ &\quad \left. \times \mathcal{B}_W \left(l'' - \frac{\delta l_2}{2}, -\theta' + \frac{\delta \theta_1}{2}; l', \theta' \right) \right], \end{aligned} \quad (53)$$

where the vertex operator $\hat{\mathcal{V}}$ is an integral operator: $\hat{\mathcal{V}}f(l, \theta; l', \theta'; l'', \theta'; \delta l_2, \delta \theta_1) \rightarrow (\hat{\mathcal{V}}f)(l, \theta; l', \theta')$ (note that the variables: $l'', \theta', \delta l_2$, and $\delta \theta_1$ in the function f are integrated out), and is defined as

$$\begin{aligned} (\hat{\mathcal{V}}f)(l, \theta; l', \theta') &\equiv \int \frac{dl'' d\theta'}{2\pi\hbar} \int \frac{d\delta l_1 d\delta \theta_1}{2\pi\hbar} \int \frac{d\delta l_2 d\delta \theta_2}{2\pi\hbar} \mathcal{X}(\delta l_1, \delta \theta_1; \delta l_2, \delta \theta_2) \\ &\quad \times \mathcal{C}_0 \left(l'' + \frac{\delta l_1}{2}, \theta' - \frac{\delta \theta_2}{2}; l'' - \frac{\delta l_1}{2}, -\theta' - \frac{\delta \theta_2}{2} \right) \\ &\quad \times f(l, \theta; l', \theta'; l'', \theta'; \delta l_2, \delta \theta_1), \end{aligned} \quad (54)$$

with

$$\begin{aligned} \mathcal{X}(\delta l_1, \delta \theta_1; \delta l_2, \delta \theta_2) &= J_0 \left(\frac{K \delta \theta_1 \delta \theta_2}{\hbar} \right) \\ &\quad \times \exp \left[\frac{i}{\hbar} (\delta l_1 \delta \theta_1 + \delta l_2 \delta \theta_2) \right]. \end{aligned} \quad (55)$$

In Eq. (53) we introduced the following notations:

$$\begin{aligned} l'' &\equiv \frac{1}{2} \left(\frac{l_2 + l'_3}{2} + \frac{l_3 + l'_2}{2} \right); \\ \theta'' &\equiv \frac{1}{2} \left(\frac{\theta_1 + \theta'_1}{2} - \frac{\theta_2 + \theta'_2}{2} \right), \end{aligned} \quad (56)$$

while the subscript W stands for Wigner transformation.

The phase difference of the two counterpropagating paths underlying the cooperon gives rise to the interference factor appearing in Eq. (55). Technically, it results from the different definitions of Wigner transform for the diffuson and the cooperon [see Eqs. (14) and (25)]. The minimal quantum wave packet possesses the uncertainty $\delta l_1 \delta \theta_1 \sim \hbar$ and $\delta l_2 \delta \theta_2 \sim \hbar$, as indicated in Eq. (55). Moreover, $\delta \theta_1 \delta \theta_2 \sim \hbar/K$. Such quantum wave packet determines the initial scale of the deviation of two nearby trajectories involved in the cooperon [cf. Eq. (39)].

2. Interaction vertex at the semiclassical level

Applying the general expression Eq. (53) to Eq. (41), we find

$$\begin{aligned} \delta \mathcal{D}(l, \theta; l', \theta') &= \hat{\mathcal{V}} \left[\mathcal{D}_0 \left(l, \theta; l'' + \frac{\delta l_2}{2}, \theta' + \frac{\delta \theta_1}{2} \right) (\tilde{P}_T - 1) \right. \\ &\quad \left. \times (\tilde{P} - 1) \mathcal{D}_0 \left(l'' - \frac{\delta l_2}{2}, -\theta' + \frac{\delta \theta_1}{2}; l', \theta' \right) \right]. \end{aligned} \quad (57)$$

Remarkably, this exact vertex $\delta \mathcal{D}$ is obtained without introducing any explicit regularization. In the next subsection we will show that it leads to the weak-localization correction to diffusion constant, which is similar to earlier findings for ballistic quantum dots.²⁷ In Appendix E we show that it is possible to introduce some artificial quantum disorder to QKR and the results obtained in the present work may be reproduced following the formalism of Ref. 27.

B. Weak-localization correction to diffusion constant

In this part, we show that the exact one-loop quantum correction, Eq. (57), may be cast into the conventional Hikami box structure with an additional factor due to the Lyapunov region. As a result, the one-loop correction affects the diffusion equation through a frequency-dependent renormalization of the diffusion coefficient: $D(\omega) = D_{cl} + \delta D(\omega)$. That is

$$[-i\omega - D(\omega)\nabla_l^2] \mathcal{D}_0 = \hbar \delta(l - l'). \quad (58)$$

We calculate then the quantum correction $\delta D(\omega)$ and find how it affects the angular momentum dispersion.

1. Effects of the Lyapunov instability on the interaction vertex

Since our aim is to describe the long-time phenomena, we expect that the typical scale of the angular momentum dispersion, say L_H , is large: $L_H \gg K$. Indeed, the angular momentum is randomly spread in the interval $\in [-K, K]$ in a single kick. It is thus natural to expect much broader distribution after many kicks. This consideration justifies the expansion with respect to $K\nabla_l$ (hydrodynamic approximation). With such approximation, the exact vertex can be cast into the Hikami box.

With the help of the identity $\vec{P}\mathcal{D}_0 = \mathcal{D}_0\vec{P}_T$, which is proven in Appendix B, Eq. (57) may be rewritten as

$$\begin{aligned} \delta \mathcal{D}(l, \theta; l', \theta') &= \hat{\mathcal{V}} \left\{ \left[(\tilde{P} - 1) \mathcal{D}_0 \left(l, \theta; l'' + \frac{\delta l_2}{2}, \theta' + \frac{\delta \theta_1}{2} \right) \right] \right. \\ &\quad \times \left[\mathcal{D}_0 \left(l'' - \frac{\delta l_2}{2}, -\theta' + \frac{\delta \theta_1}{2}; l', \theta' \right) \right] \\ &\quad \left. \times (\tilde{P}_T - 1) \right\}. \end{aligned} \quad (59)$$

Since $\mathcal{X}\mathcal{C}_0$ has no dependence on (l'', θ') , Eq. (59) contains

$$\begin{aligned} I &= \int \frac{dl'' d\theta'}{2\pi\hbar} \mathcal{D}_0 \left(l, \theta; l'' + \frac{\delta l_2}{2}, \theta' + \frac{\delta \theta_1}{2} \right) \\ &\quad \times \mathcal{D}_0 \left(l'' - \frac{\delta l_2}{2}, -\theta' + \frac{\delta \theta_1}{2}; l', \theta' \right). \end{aligned} \quad (60)$$

To proceed further, we employ the following relation:

$$\mathcal{D}_0(l, \theta; l', \theta') = \mathcal{D}_0(l', -\theta'; l, -\theta), \quad (61)$$

which reflects the time reversibility; its derivation is given in Appendix B. The remaining procedure is fully analogous to calculation of the cooperon developed in Sec. III C. The only difference is in the boundary conditions. In fact, the angular deviation of two traveling nearby trajectories, $\delta\theta$, reaches a classical size $|\delta\theta'| \lesssim 1$ at some point in the phase space, say (l_{n_c}, θ_{n_c}) . The later evolutions are independent. That is, the two diffusons become self-averaging over the (random) paths connecting two remote ends, resulting in the factorization of the two averaged diffusons as

$$\begin{aligned} & \left[\mathcal{D}_0\left(l'' + \frac{\delta l_2}{2}, -\theta' - \frac{\delta\theta_1}{2}; l, -\theta\right) \right. \\ & \quad \left. \times \mathcal{D}_0\left(l'' - \frac{\delta l_2}{2}, -\theta' + \frac{\delta\theta_1}{2}; l', \theta'\right) \right] \\ & \rightarrow \left\langle \mathcal{D}_0\left(l_1 + \frac{\delta l''}{2}, -\theta_1 - \frac{\delta\theta''}{2}; l, -\theta\right) \right\rangle \\ & \quad \times \left\langle \mathcal{D}_0\left(l_1 - \frac{\delta l''}{2}, -\theta_1 + \frac{\delta\theta''}{2}; l', \theta'\right) \right\rangle. \quad (62) \end{aligned}$$

Taking this boundary condition into account, we obtain

$$\begin{aligned} I = \mathcal{W}_D(2\omega) & \int \frac{dl_1 d\theta_1}{2\pi\hbar} \left\langle \mathcal{D}_0\left(l, \theta; l_1 + \frac{\delta l''}{2}, \theta_1 + \frac{\delta\theta''}{2}\right) \right\rangle \\ & \times \left\langle \mathcal{D}_0\left(l_1 - \frac{\delta l''}{2}, -\theta_1 + \frac{\delta\theta''}{2}; l', \theta'\right) \right\rangle. \quad (63) \end{aligned}$$

Note that the two intermediate angular momenta deviate as $\delta l''/2$. Such deviation is unimportant because the distribution with respect to the angular momentum fluctuates over the large scale $L_H \gg K \gg \delta l''/2$. In Eq. (63) $\mathcal{W}_D(\omega)$ is the same as $\mathcal{W}_C(\omega)$, except that t^C is replaced by (with the logarithmic accuracy)

$$t^D = \frac{1}{\lambda} \left| \ln \frac{1}{\sqrt{\delta\theta^2 + \delta l^2/K^2}} \right|, \quad (64)$$

where $\delta\theta$ is the initial angular separation of two nearby trajectories involved in the diffuson side of the Lyapunov region. It is determined by the minimal quantum wave packet, i.e., by \mathcal{X} [see Eq. (55)]. We then substitute Eqs. (54) and (63) into Eq. (59), and restore the operator under the average. As a result, we obtain

$$\begin{aligned} \delta\mathcal{D}(l, \theta; l', \theta') = \mathcal{V} & \int \frac{dl_1 d\theta_1}{2\pi\hbar} \left\langle \left\langle \mathcal{D}_0\left(l, \theta; l_1 + \frac{\delta l''}{2}, \theta_1 + \frac{\delta\theta''}{2}\right) \right. \right. \\ & \quad \left. \times (\tilde{P}_T - 1) \right\rangle \left\langle (\tilde{P} - 1) \mathcal{D}_0\left(l_1 - \frac{\delta l''}{2}, -\theta_1 \right. \right. \\ & \quad \left. \left. + \frac{\delta\theta''}{2}; l', \theta'\right) \right\rangle \left. \right\rangle, \quad (65) \end{aligned}$$

where

$$\begin{aligned} \mathcal{V} & \equiv \int \frac{d\delta l_1 d\delta\theta_1}{2\pi\hbar} \int \frac{d\delta l_2 d\delta\theta_2}{2\pi\hbar} \mathcal{W}_D(2\omega) \mathcal{X}(\delta l_1, \delta\theta_1; \delta l_2, \delta\theta_2) \\ & \quad \times C_0\left(l'' + \frac{\delta l_1}{2}, \theta' - \frac{\delta\theta_2}{2}; l'' - \frac{\delta l_1}{2}, -\theta' - \frac{\delta\theta_2}{2}\right). \quad (66) \end{aligned}$$

Here, \mathcal{V} may be regarded as the renormalized interaction strength. To further calculate it, we substitute Eq. (40) into Eq. (66). As a result, \mathcal{V} is found to be

$$\mathcal{V} = \Gamma(\omega) \int \frac{d\varphi}{2\pi - i\omega + D_{cl}\varphi^2}, \quad (67)$$

where

$$\begin{aligned} \Gamma(\omega) & \equiv \int \frac{d\delta l_1 d\delta\theta_1}{2\pi\hbar} \int \frac{d\delta l_2 d\delta\theta_2}{2\pi\hbar} \mathcal{W}_C(2\omega) \mathcal{W}_D(2\omega) \mathcal{X} \\ & = \int \frac{d\delta l_1 d\delta\theta_1}{2\pi\hbar} \int \frac{d\delta l_2 d\delta\theta_2}{2\pi\hbar} \\ & \quad \times J_0\left(\frac{K\delta\theta_1\delta\theta_2}{\hbar}\right) \exp\left[\frac{i}{\hbar}(\delta l_1\delta\theta_1 + \delta l_2\delta\theta_2)\right] \\ & \quad \times \exp\left[\left(2i\omega - \frac{2\omega^2\lambda_2}{\lambda^2}\right)|z_1 + z_2|\right], \quad (68) \end{aligned}$$

with

$$z_1 = \ln \sqrt{\delta\theta_1^2 + \delta l_1^2/K^2}, \quad z_2 = \ln \sqrt{\delta\theta_2^2 + \delta l_2^2/K^2}. \quad (69)$$

Rescaling $\delta\theta_{1,2}$ and $\delta l_{1,2}$ as

$$\delta\theta_{1,2} \rightarrow \delta\theta_{1,2}/\sqrt{\hbar/K}, \quad \delta l_{1,2} \rightarrow \delta l_{1,2}/\sqrt{\hbar K} \quad (70)$$

leads to

$$\Gamma(\omega) = \exp\left(4i\omega t_E - \frac{4\omega^2\lambda_2 t_E}{\lambda^2}\right) F(\omega), \quad (71)$$

where $F(\omega)$ is

$$\begin{aligned} F(\omega) & = \int \frac{dl_1 d\theta_1}{2\pi} \int \frac{dl_2 d\theta_2}{2\pi} J_0(\theta_1\theta_2) \exp[i(l_1\theta_1 + l_2\theta_2)] \\ & \quad \times \exp\left[\left(2i\omega - \frac{2\omega^2\lambda_2}{\lambda^2}\right)|\tilde{z}_1 + \tilde{z}_2|\right], \\ & \quad \tilde{z}_1 = \ln \sqrt{\theta_1^2 + l_1^2}, \quad \tilde{z}_2 = \ln \sqrt{\theta_2^2 + l_2^2}. \quad (72) \end{aligned}$$

Here, $t_E = (t^C + t^D)/2$, which is Eq. (2). Since $\tilde{z}_{1,2} \sim 1$, in the limit $\omega, \omega\lambda_2/\lambda^2 \ll 1$, the last exponent in Eq. (72) may be considered to be 1. As a result, $F(\omega) = 1$. Thus, we obtain

$$\Gamma(\omega) = \exp\left(4i\omega t_E - \frac{4\omega^2\lambda_2 t_E}{\lambda^2}\right). \quad (73)$$

We point out that the position of the minimal wave packet—Hikami box *cannot* be exactly located within the Lyapunov region. Indeed, this is reflected in the fact that the total duration within the Lyapunov region, i.e., $4t_E$, actually does *not* depend on the exact boundary between cooperon

and diffuson. Such feature originates from the chaotic nature of the classical motion in the phase space. At each full travel, the initial deviation, $\delta l_{1,2}$ ($\delta\theta_{1,2}$) with respect to the reference trajectory expands in the backward (forward) time direction. Eventually $\delta l_1 \delta\theta_1$ ($\delta l_2 \delta\theta_2$) reaches some classical action K (the typical scale of the classical action). Therefore, the total duration is

$$4t_E = \frac{1}{\lambda} \ln \frac{K}{\delta l_1 \delta\theta_1} + \frac{1}{\lambda} \ln \frac{K}{\delta l_2 \delta\theta_2}. \quad (74)$$

Taking into account the uncertainty relation $\delta l_1 \delta\theta_1 \approx \delta l_2 \delta\theta_2 \approx \hbar$, we find the total duration to be $4t_E = 4\lambda^{-1} \ln \sqrt{K/\hbar}$.

2. Frequency-dependent diffusion coefficient

The renormalized interaction vertex, Eq. (65), may be further cast into the conventional (diffusive) Hikami box upon further simplifications. As discussed above, the hydrodynamic expansion may be performed because $K/L_H \ll 1$. This allows the further simplification of Eq. (65). One finds to the first order in the hydrodynamic expansion

$$\begin{aligned} \left\langle \tilde{P} \mathcal{D}_0 \left(l_1 - \frac{\delta l''}{2}, -\theta_1 + \frac{\delta\theta''}{2}; l', \theta' \right) \right\rangle &= \left\langle \mathcal{D}_0 \left(l_1 - \frac{\delta l''}{2} + K \sin \left[\theta_1 - \frac{\delta\theta''}{2} + l_1 - \frac{\delta l''}{2} \right], - \left[\theta_1 - \frac{\delta\theta''}{2} + l_1 - \frac{\delta l''}{2} \right]; l', \theta' \right) \right\rangle \\ &\approx \left\langle \left[1 + K \sin \left(\theta_1 - \frac{\delta\theta''}{2} + l_1 - \frac{\delta l''}{2} \right) \nabla_{l_1} \right] \mathcal{D}_0 \left(l_1 - \frac{\delta l''}{2}, - \left[\theta_1 - \frac{\delta\theta''}{2} + l_1 - \frac{\delta l''}{2} \right]; l', \theta' \right) \right\rangle \\ &\approx \left[1 + K \sin \left(\theta_1 - \frac{\delta\theta''}{2} + l_1 - \frac{\delta l''}{2} \right) \nabla_{l_1} \right] \left\langle \mathcal{D}_0 \left(l_1 - \frac{\delta l''}{2}, - \left[\theta_1 - \frac{\delta\theta''}{2} + l_1 - \frac{\delta l''}{2} \right]; l', \theta' \right) \right\rangle. \end{aligned} \quad (75)$$

The last line results from the fact that $\langle \mathcal{D}_0 \rangle$ has weaker dependence on the angle compared to the sinusoidal term for sufficiently large K . Similarly

$$\begin{aligned} \left\langle \mathcal{D}_0 \left(l, \theta; l_1 + \frac{\delta l''}{2}, \theta_1 + \frac{\delta\theta''}{2} \right) \tilde{P}_T \right\rangle &\approx \left[1 + K \sin \left(\theta_1 + \frac{\delta\theta''}{2} + l_1 + \frac{\delta l''}{2} \right) \nabla_{l_1} \right] \\ &\times \left\langle \mathcal{D}_0 \left(l, \theta; l_1 + \frac{\delta l''}{2}, \theta_1 + \frac{\delta\theta''}{2} + l_1 - \frac{\delta l''}{2} \right) \right\rangle. \end{aligned} \quad (76)$$

On the other hand, by shifting the overall angle factor

$$\begin{aligned} \int \frac{dl_1 d\theta_1}{2\pi\hbar} \left\langle \mathcal{D}_0 \left(l_1 - \frac{\delta l''}{2}, - \left[\theta_1 - \frac{\delta\theta''}{2} + l_1 - \frac{\delta l''}{2} \right]; l', \theta' \right) \right\rangle &\times \left\langle \mathcal{D}_0 \left(l, \theta; l_1 + \frac{\delta l''}{2}, \theta_1 + \frac{\delta\theta''}{2} + l_1 - \frac{\delta l''}{2} \right) \right\rangle \\ &= \int \frac{dl_1 d\theta_1}{2\pi\hbar} \left\langle \mathcal{D}_0 \left(l_1 + \frac{\delta l''}{2}, - \theta_1 + \frac{\delta\theta''}{2}; l', \theta' \right) \right\rangle \\ &\times \left\langle \mathcal{D}_0 \left(l, \theta; l_1 + \frac{\delta l''}{2}, \theta_1 + \frac{\delta\theta''}{2} \right) \right\rangle. \end{aligned} \quad (77)$$

This arises from the uniform distribution with respect to the common angle in the product of the two averaged diffusons.

We then substitute these two expansions, Eqs. (75) and (76), as well as Eq. (77), into Eq. (65). For sufficiently large

K , the sinusoidal term is quasirandom and may be averaged over the angular region $[0, 2\pi]$. As a result, the linear term in the hydrodynamic expansion does not survive upon this averaging, and the second-order term must be kept. Finally, we obtain

$$\begin{aligned} \delta \mathcal{D}(l, \theta; l', \theta') &= \nu \int \frac{dl_1 d\theta_1}{2\pi\hbar} K^2 \left\langle \sin \left(\theta_1 - \frac{\delta\theta''}{2} \right) \right. \\ &\times \left. \sin \left(\theta_1 + \frac{\delta\theta''}{2} \right) \right\rangle \nabla_{l_1'} \nabla_{l_1''} \\ &\times \left[\left\langle \mathcal{D}_0 \left(l, \theta; l_1' + \frac{\delta l''}{2}, \theta_1 + \frac{\delta\theta''}{2} \right) \right\rangle \right. \\ &\times \left. \left\langle \mathcal{D}_0 \left(l_1'' - \frac{\delta l''}{2}, - \theta_1 + \frac{\delta\theta''}{2}; l', \theta' \right) \right\rangle \right] \Big|_{l_1' = l_1'' = l_1}. \end{aligned} \quad (78)$$

Since $\delta\theta'' \ll 1 \sim \theta_1$

$$K^2 \left\langle \sin \left(\theta_1 - \frac{\delta\theta''}{2} \right) \sin \left(\theta_1 + \frac{\delta\theta''}{2} \right) \right\rangle \approx K^2 \langle \sin^2 \theta_1 \rangle = 2D_{cl}. \quad (79)$$

On the other hand, the diffuson is smooth over the scale $\sim K$; hence, we may also drop out $\delta l''/2$ in Eq. (78). Finally $\delta \mathcal{D}$ is cast into

$$\begin{aligned} \delta D(l, \theta; l', \theta') &= 2\mathcal{V} \int \frac{dl_1 d\theta_1}{2\pi\hbar} D_{cl} \nabla_{l'_1} \nabla_{l''_1} [\langle \mathcal{D}_0(l, \theta; l'_1, \theta_1) \rangle \\ &\times \langle \mathcal{D}_0(l''_1, -\theta_1; l', \theta') \rangle] |_{l'_1=l''_1=l_1}. \end{aligned} \quad (80)$$

In the calculation of the Hikami box given above, we set $\tau_c=1$. As a result, the diffusion coefficient appearing in Eq. (80) is $D_{cl}=K^2/4$. However, we emphasize that if more kicks are reserved for the Hikami box, i.e., \hat{P}^n , $n>1$, then the diffusion coefficient will acquire the same higher-order corrections as described by Eq. (24). Therefore, the assumption $\tau_c=1$ does not restrict generality of the result.

With the angle averaged out, diffusion is retrieved. As a result, the one-loop correction, Eq. (80), is simplified as

$$\begin{aligned} \delta \mathcal{D}_0(l, l') &= \hbar^{-1} \int dl_1 \mathcal{V} D_{cl} [\nabla_{l'_1}^2 + \nabla_{l''_1}^2] \\ &\times [\mathcal{D}_0(l, l'_1) \mathcal{D}_0(l''_1, l')] |_{l'_1=l''_1=l_1}. \end{aligned} \quad (81)$$

Denote the Fourier transform of $\mathcal{D}_0(l, l')$, with respect to $l-l'$ as $\mathcal{D}_0(\varphi; \omega)$. Substituting Eq. (67) into Eq. (81), we find the Fourier transform one-loop correction

$$\delta \mathcal{D}_0(\varphi; \omega) = \frac{\hbar \Gamma(\omega) D_{cl} \varphi^2}{(-i\omega + D_{cl} \varphi^2)^2} \int \frac{d\phi}{\pi - i\omega + D_{cl} \phi^2}, \quad (82)$$

which leads to the one-loop quantum correction to the diffusion coefficient as

$$\delta D(\omega) = -\frac{\hbar D_{cl}}{\pi} \Gamma(\omega) \int \frac{d\phi}{-i\omega + D_{cl} \phi^2}. \quad (83)$$

3. Dispersion function

One may express the time evolution of the angular momentum dispersion as $\delta \langle l^2(t) \rangle \equiv \langle (l(t) - l(0))^2 \rangle$ in terms of the frequency-dependent diffusion coefficient. In fact, by averaging over the angle, we may write $\delta \langle l^2(t) \rangle$ as

$$\begin{aligned} \delta \langle l^2(t) \rangle &= \sum_l (l-l')^2 [\mathcal{D}_0(l, l'; t) - \mathcal{D}_0(l, l'; 0)] \\ &= -\frac{\partial^2}{\partial \varphi^2} [\mathcal{D}_0(\varphi; t) - \mathcal{D}_0(\varphi; 0)] |_{\varphi \rightarrow 0}. \end{aligned} \quad (84)$$

Substituting Eq. (58) into it, we obtain

$$\delta \langle l^2(t) \rangle = \int_{-\infty}^{\infty} \frac{d\omega}{\pi} \frac{1 - e^{-i\omega t}}{\omega^2} D(\omega). \quad (85)$$

For sufficiently large K , one may ignore the fluctuation of λ , i.e., set $\lambda_2=0$. Consequently, in the leading order in \hbar the momentum dispersion is found to be

$$\delta \langle l^2(t) \rangle = 2D_{cl} t - \frac{8\hbar \sqrt{D_{cl}}}{3\sqrt{\pi}} \theta(t - 4t_E) (t - 4t_E)^{3/2}, \quad (86)$$

where $\theta(t)$ is the step function (long-dashed line in Fig. 2). The singularity at $t=4t_E$ is rounded by the Ehrenfest time fluctuations arising from finite λ_2 (full line in Fig. 2). Sub-

stituting Eqs. (73) and (83) into Eq. (85), we arrive at

$$\begin{aligned} \delta \langle l^2(t) \rangle - 2D_{cl} t &= -\frac{4\hbar \sqrt{D_{cl}}}{3\pi} (\delta t_E)^{3/2} \int_{-\infty}^{\infty} d\tau \theta\left(\frac{t-4t_E}{\delta t_E} - \tau\right) \\ &\times \left(\frac{t-4t_E}{\delta t_E} - \tau\right)^{3/2} e^{-\tau^2/16}, \end{aligned} \quad (87)$$

where $\delta t_E = \sqrt{\lambda_2 t_E / \lambda^2}$. As a result

$$\delta \langle l^2(t) \rangle = 2D_{cl} t - \frac{\Gamma\left(\frac{5}{4}\right) \hbar}{3\pi/64} \sqrt{D_{cl}} (\delta t_E)^{3/2} f\left(\frac{4t_E - t}{\delta t_E}\right), \quad (88)$$

where $f(0)=1$ and

$$f(x) = \begin{cases} \frac{8\sqrt{2}\Gamma\left(\frac{7}{2}\right)}{\Gamma\left(\frac{5}{4}\right)} x^{-5/2} e^{-x^2/16} & \text{for } x \gg 1. \\ \frac{1}{8\Gamma\left(\frac{5}{4}\right)} (-x)^{3/2} & \text{for } -x \gg 1. \end{cases} \quad (89)$$

This result completes the calculations of the one-loop weak-localization correction.

V. WEAK-DYNAMICAL LOCALIZATION OF QKR WITH BROKEN TIME-REVERSAL SYMMETRY

To exploit further similarities and differences of the dynamical localization of the QKR and the Anderson localization, we discuss here effects of breaking the time-reversal symmetry (TRS). In the case of Anderson localization in a random potential the TRS may be broken, for example, by a static magnetic field. The latter provides different phases for clockwise and anticlockwise propagating trajectories, thus destroying the systematic interference correction discussed in Sec. II. It does not, though, ruin, the Anderson localization completely. Indeed, higher-order corrections (the minimum possible is the two-loop one) may be interpreted as interference of trajectories traveling the loops in the same direction only (diffuson-only diagrams with no cooperons). The static magnetic field does not affect such diagrams. As a result, the Anderson localization exists even in this case, albeit with somewhat larger localization length.

It has thus long been of interest to show that an analogous phenomenon exists for the QKR as well.^{23,34,39-41} Our additional motivation comes from consideration of the Lyapunov regime and its sensitivity to the TRS breaking. In particular, the one-loop (TRS-invariant) correction was found to be delayed by $4t_E$. Does this time interval remain to be protected against perturbative corrections in higher loop processes? Is the delay time still the same? These questions are of particular interest if and when the leading one-loop correction is destroyed by TRS breaking.

To answer these questions, we investigate the model, described by the following Hamiltonian:

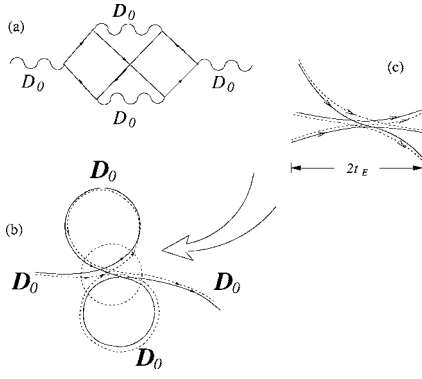


FIG. 6. The leading quantum correction to the density-density correlator in the absence of the time-reversal symmetry (6-leg Hikami box): (a) two-loop weak localization diagram; (b) its image in the momentum space; (c) Hikami box.

$$\hat{H} = \frac{\hat{p}^2}{2} + K \sum_n [\cos \hat{\theta} \delta(t - 2n) + \cos(\hat{\theta} + \Phi) \delta(t - (2n + 1))]. \quad (90)$$

Here, the time-reversal symmetry is broken for generic Φ except for $\Phi = 0, \pi$. First, we analyze suppression of the cooperon (and thus the one-loop diagram) arising from Φ . We then calculate the two-loop correction. In contrast to the one-loop correction, the two-loop one is robust against Φ because it contains (among others) diagrams without the cooperons. If the TRS is broken, the long-time correction is given by the two-loop diagrams depicted in Fig. 6 and Fig. 7,⁴²⁻⁴⁴ which involve the 6-leg and 4-leg Hikami box, respectively. They differ from Fig. 1 in that the two interfering paths propagate together in the *same* direction, except inside the Hikami box, where they switch from one to the other. Due to such geometry, the two-loop correction is not sensitive to Φ . It requires several successive traveling (three for Fig. 6, while four for Fig. 7) through the Lyapunov region (each taken $2t_E$ time). We show thus that the weak localization corrections, given by this diagram, are delayed by $6t_E$ and $8t_E$,⁴⁴ respectively.

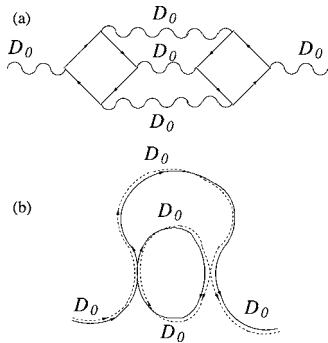


FIG. 7. The leading quantum correction to the density-density correlator in the absence of the time-reversal symmetry (4-leg Hikami box): (a) two-loop weak localization diagram; (b) its image in the momentum space.

A. Suppression of one-loop correction

In the modified KR model, Eq. (90), the period is doubled and includes two kicks. The effective kicking operator appearing in the one-step evolution operator \hat{U} [cf. Eq. (13)] is replaced by

$$\hat{\mathcal{P}}'_J \equiv \exp \left[i \frac{K}{\hbar} \cos \hat{\theta} \right] \exp \left[\frac{i \hat{p}^2}{2\hbar} \right] \exp \left[i \frac{K}{\hbar} \cos(\hat{\theta} + \Phi) \right]. \quad (91)$$

In the angular momentum representation, the matrix elements read as

$$\begin{aligned} \langle l_+ | \hat{\mathcal{P}}'_J | l'_+ \rangle &= \sum_{l_1} \int \frac{d\theta_+}{2\pi} \int \frac{d\theta_1}{2\pi} e^{-i(l_1/\hbar)\theta_+} e^{i(l_+ - l_1)/\hbar} e^{i(K/\hbar)\cos \theta_+} \\ &\times e^{i l_1^2 / 2\hbar} e^{-i(l_1/\hbar)\theta_1} e^{i(K/\hbar)\cos(\theta_1 + \Phi)}, \end{aligned} \quad (92)$$

while its complex conjugation is

$$\begin{aligned} \langle l_- | \hat{\mathcal{P}}'_J | l'_- \rangle^* &= \sum_{l'_1} \int \frac{d\theta_-}{2\pi} \int \frac{d\theta'_1}{2\pi} e^{i(l_1/\hbar)\theta_-} e^{-i(l_1 - l'_1)/\hbar} e^{-i(K/\hbar)\cos \theta_-} \\ &\times e^{-i(l_1'^2 / 2\hbar)} e^{i(l_1'/\hbar)\theta'_1} e^{-i(K/\hbar)\cos(\theta'_1 + \Phi)}. \end{aligned} \quad (93)$$

First, we investigate the effects of Φ on the diffusive parts of diffusons and cooperons. To simplify the discussion we assume that K is sufficiently large, implying that the memory about the angle is lost after a single kick. To find the self-energy of the diffuson, we replace the kicking operator J in Eq. (20) with $\hat{\mathcal{P}}'_J$. Then, we insert Eqs. (92) and (93) into it, putting $l_1 = l'_1$. Consequently, the diffusive pole is retrieved as $\theta_+ - \theta_- = \theta_1 - \theta'_1 \equiv \hbar\varphi$, and the self-energy of the diffuson is

$$\langle l | \hat{\mathcal{P}}'_J | l'' \rangle \langle l | \hat{\mathcal{P}}'_J | l'' \rangle^* = \int \frac{d\varphi}{2\pi} J_0^2 \left(\frac{2K}{\hbar} \sin \frac{\hbar\varphi}{2} \right) e^{i\varphi(l - l'')}. \quad (94)$$

This expression demonstrates the period doubling (Bessel function is squared) and implies that the diffuson is not affected by Φ .

For the diffusive cooperon, the self-energy is $\langle l | \hat{\mathcal{P}}'_J | l'' \rangle \times \langle l'' | \hat{\mathcal{P}}'_J | l \rangle^*$. Inserting Eqs. (92) and (93) into it, and putting $l_1 = l'_1$, we find that the Cooperon has diffusive pole at

$$\theta_+ + \theta_- = \theta_1 + \theta'_1 \equiv \hbar\varphi, \quad (95)$$

and the self-energy is

$$\begin{aligned} \langle l | \hat{\mathcal{P}}'_J | l'' \rangle \langle l'' | \hat{\mathcal{P}}'_J | l \rangle^* &= \int \frac{d\varphi}{2\pi} e^{i\varphi(l - l'')} J_0 \left(\frac{2K}{\hbar} \sin \frac{\hbar\varphi}{2} \right) \\ &\times J_0 \left[\frac{2K}{\hbar} \sin \left(\frac{\hbar\varphi}{2} + \Phi \right) \right]. \end{aligned} \quad (96)$$

In the derivation above, we used the fact that for sufficiently large K , $(\theta_+ - \theta_-)/2$ and $(\theta_1 - \theta'_1)/2$ is quasirandom and the self-averaging may be performed. With the Fourier transform

with respect to time, the self-energy leads to the diffusive cooperon of the form

$$\langle C_0(l, \theta; l', -\theta'; \omega) \rangle = \bar{\kappa} \int \frac{d\varphi}{2\pi} \frac{1}{-i\omega + \frac{1}{2}D_{cl}[\varphi^2 + (\varphi + 2\Phi/\bar{\kappa})^2]} \quad (97)$$

in the limit $K\varphi, K\Phi/\bar{\kappa} \ll 1$. Here, $|l-l'| \leq K, |\theta-\theta'| \sim 1$. According to Eq. (97) the relaxation time of the cooperon is $\tau_\Phi = (D_{cl}\Phi^2/\bar{\kappa}^2)^{-1}$. At $\Phi \gtrsim \bar{\kappa}/\sqrt{D_{cl}} \sim \bar{\kappa}/K, \tau_\Phi \sim 1$ the cooperon is completely suppressed.

The propagation in the Lyapunov region involves deterministic motion, which is also affected by Φ . Therefore, the Lyapunov exponent λ , as well as its fluctuations λ_2 , acquires some Φ dependence. However, since the propagator has no dependence on the center of mass, the functional form of $\mathcal{W}_{C,D}(2\omega)$ remains unchanged. Thus, the procedure of Sec. IV B can be employed to show that the dispersion function is given by

$$\delta\langle l^2(t) \rangle = 2D_{cl}t - \frac{4\bar{\kappa}\sqrt{D_{cl}}}{\sqrt{\pi}} \theta(t-4t_E) \tau_\Phi^{3/2} h\left(\frac{t-4t_E}{\tau_\Phi}\right), \quad (98)$$

where the function $h(x)$ is

$$h(x) = \int_0^x dy_1 \int_0^{\sqrt{y_1}} dy_2 e^{-y_2^2}. \quad (99)$$

Notice that here t_E is a function of Φ , i.e., $t_E(\Phi) = \lambda(\Phi)^{-1} \ln \sqrt{K/\bar{\kappa}}$. For simplicity, we neglected the fluctuations of $\lambda(\Phi)$, i.e., we set $\lambda_2=0$. In the region $t-4t_E \gg \tau_\Phi$, the one-loop correction is exponentially suppressed. One is required, thus, to consider the higher-loop corrections. The two-loop corrections (Fig. 6 and Fig. 7) give the leading weak-dynamical localization corrections.

B. Two-loop correction

In principle, the technique developed at the one-loop level can be employed to treat the two-loop case. However, this is technically quite involved and is not discussed here. To read out the frequency-dependent diffusion coefficient in an economical way, let us renormalize the standard results of the weak localization²⁰ with an appropriate t_E -dependent factor [this procedure indeed is transparent at the one-loop level, Eq. (83)]. The renormalization factors for the two-loop geometries (see Fig. 6 and Fig. 7) were calculated before^{28,44} in the context of chaotic quantum billiards. They are $\Gamma_3(\omega)$ and $\Gamma^2(\omega)$, respectively, where

$$\Gamma_3(\omega) = \exp\left(6i\omega t_E - \frac{9\omega^2 \lambda_2 t_E}{\lambda^2}\right). \quad (100)$$

Adopting the analogy between chaotic quantum billiards and the QKR, verified above on the one-loop level, one finds for the two-loop frequency-dependent correction to the diffusion coefficient

$$\delta D(\omega) = -2\bar{\kappa}D_{cl}[\Gamma_3(\omega) - 2\Gamma^2(\omega)] \left[\int \frac{d\varphi}{2\pi(-i\omega + D_{cl}\varphi^2)} \right]^2. \quad (101)$$

As a result, the leading correction to the momentum dispersion in the case of broken TRS is given by

$$\delta\langle l^2(t) \rangle = 2D_{cl}t - \frac{1}{4}\bar{\kappa}^2 \theta(t-6t_E)(t-6t_E)^2 + \frac{1}{2}\bar{\kappa}^2 \theta(t-8t_E) \times (t-8t_E)^2. \quad (102)$$

Again we ignore λ_2 for simplicity. To develop the two-loop geometry, a minimal quantum wave packet must take time t_E to expand into some macroscopic size, and vice versa. Within the logarithmic accuracy t_E appearing here is the same as that in the one-loop correction. Therefore, the duration for a full travel through the Lyapunov region remains the same as the one-loop case, namely $2t_E$ time. The two-loop geometries (see Fig. 6 and Fig. 7) involve three and four successive visits, respectively. As a result the weak-localization corrections, given by these two diagrams, are delayed by $6t_E$ and $8t_E$, respectively.⁴⁴

VI. OBSERVATIONS OF CLASSICAL-TO-QUANTUM CROSSOVER IN REALISTIC DRIVEN SYSTEMS

In this section, we discuss some possibilities for experimental observations of the predicted t_E dependence of the classical-to-quantum crossover. The quantity to be measured is the dispersion function $\delta\langle l^2(t) \rangle$.

A. Energy growth in cold atomic gases

In the 90's unprecedented degree of control reached in experiments with ultracold atomic gases⁴⁵ allowed investigation of various fundamental quantum phenomena. The advent of laser-cooled atomic gases and standing wave optical pulses^{2,3,8} has opened the door to study quantum chaos experimentally. In an insightful paper,⁴⁶ Graham, Schlautmann, and Zoller pointed out that atom optics may serve as a testing ground for quantum chaos. Shortly after, the idea came into realization with sodium atoms being cooled and trapped using the magneto-optical trap, subjected to a phase-modulated standing wave.⁴⁷ Later on, a realization of the QKR in atom optics was accomplished with the phase-modulated standing wave replaced by a pulsed standing wave.²

In an atom-optical experiment, typically 10^6 sodium or cesium atoms are trapped and cooled down to $10 \mu\text{K}$ using the conventional magneto-optical trap. After turning off the trapping fields, two linearly polarized, counterpropagated optical beams with the frequency ω_L are switched on, creating a spatially periodic potential: $V_0 \cos(2k_L x)$. Here, $k_L = \omega_L/c$ is the laser wave number. Such optical lattice is controlled by the acousto-optical modulator as a pulse sequence with a profile $f(t)$. The pulse length τ_p may be much smaller than the period T . The atomic cloud exposed to this pulsed optical lattice thereby experiences a series of kicks. The evolution of the atomic momenta distribution is monitored after a certain number of kicks.

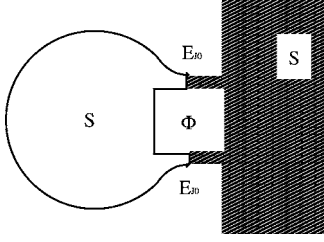


FIG. 8. The scheme of the driven Josephson grain: a superconducting dot (left) is coupled to a bulk superconductor (right) via a SQUID loop (middle). The flux Φ piercing the SQUID loop is time dependent. It effectively modifies the bare Josephson coupling E_{J0} of the two junctions.

In experiments, the laser detuning $\Delta_L \equiv \omega_L - \omega_0$ from the resonance frequency ω_0 is large compared to the excited-state decay rate. The dipole force due to the Stark effect leads to the spatially dependent shift of atomic levels. This results in an effective periodic potential imposed on the atomic cloud. One may model the center-of-mass motion of atoms with the single-particle time-dependent Hamiltonian as

$$\hat{H} = \frac{\hat{p}^2}{2m} + V_0 \cos(2k_L \hat{x}) \sum_{n=0}^N f(t - nT), \quad (103)$$

where m is the atomic mass, and k_L is the laser wave number. The effective potential, V_0 , is determined by the maximum Rabi frequency Ω as $V_0 = \hbar \Omega^2 / 8 \Delta_L$. The position \hat{x} , and the momentum \hat{p} operators are canonically conjugated: $[\hat{x}, \hat{p}] = i\hbar$. The effective kicking strength K , and the Planck constant \hbar may be expressed then as

$$K = 8\omega_r T^2 \tau_p V_0 / \hbar, \quad \hbar = 8\omega_r T, \quad (104)$$

with the recoil frequency $\omega_r = \hbar k_L^2 / 2m$. With the rescaling $x \rightarrow \theta \equiv 2k_L x$, $p \rightarrow l \equiv (\hbar / 2k_L) p$, $t \rightarrow t/T$, $f(t) \rightarrow f(t) / \tau_p$, $H \rightarrow (\hbar k_L / \hbar) H$, one casts the Hamiltonian into Eq. (1) in the limit $\tau_p / T \rightarrow 0$ (with K fixed).⁴⁸

So far, many experimental efforts^{2,8} have been focused on the parameter range where $\hbar \geq 2$, and thus $t_E \approx 1$. The dynamical localization has been observed as the saturation of the time-dependent momentum distribution width (i.e., energy absorption). To extract accurately the t_E -dependent crossover, one needs a large separation between the relevant time scales: $1 < t_E < t_L$. This requires decreasing \hbar down to 0.1–1, which we hope to be soon within reach for cold atomic gases experiments.^{32,33}

B. Charge fluctuations on Josephson grains

The experimental realization of the QKR also may be feasible in experiments involving small nonequilibrium superconducting systems. One example is a small superconductive dot in contact with a bulk superconductor through two Josephson junctions (see Fig. 8).⁴⁹ The bare Josephson coupling, E_{J0} , is modulated by the external magnetic flux threading the SQUID loop:^{50–52} $E_J = E_{J0} |\cos(\pi B A_{loop} / \Phi_0)|$,

where A_{loop} is the area of the SQUID loop, and $\Phi_0 \equiv h/2e$ is the superconducting flux quantum. If B is modulated in a meander way, with the pulse length much smaller than the period T , the system may be modeled by the Hamiltonian

$$\hat{H} = \frac{(\hat{Q} - CV_g)^2}{2C} - \bar{E}_J T \cos \theta \sum_n \delta(t - nT). \quad (105)$$

Here, $\hat{\theta}$ and \hat{Q} are the relative phase of the superconducting order parameter on the grain, and its charge, correspondingly. They are canonically conjugated: $[\hat{\theta}, \hat{Q}] = 2ei$. In Eq. (105) C is the capacitance, V_g is the gate voltage, and \bar{E}_J is the time-average Josephson coupling. Making change of the variables: $\hat{Q} \rightarrow \hat{l} \equiv \hbar \hat{Q} / 2e$ and rescaling the relevant quantities as $t \rightarrow t/T$, $\hat{H} \rightarrow 8E_c T^2 \hat{H} / \hbar^2$, and $CV_g \rightarrow v_g \equiv \hbar CV_g / 2e$ ($E_c = e^2 / 2C$), we cast the Hamiltonian above into QKR

$$\hat{H} = \frac{1}{2} (\hat{l} - v_g)^2 - K \cos \theta \sum_n \delta(t - n). \quad (106)$$

Note that the sign difference in the kicking term is immaterial. Here, the effective Planck's constant and kicking strength are

$$\hbar = 8E_c T / \hbar, \quad K = 8E_c \bar{E}_J T^2 / \hbar^2, \quad (107)$$

respectively.

The charge fluctuations are described by the charge dispersion: $\sim \delta \langle l^2(t) \rangle$. For sufficiently large K and $t < 4t_E$ it is expected to increase linearly in time. At $t \geq 4t_E$, it should deviate from the linearity.²⁹ At longer time, $t \gg 4t_E$, the $t^{3/2}$ power-law correction develops following the conventional weak-localization theory.^{1,18,19} This signals the onset of the localization phenomena. Eventually, at $t \sim D_{cl} / \hbar_2 \gg t_E$ the charge fluctuations saturate and do not grow any more upon further kicking.

C. Charge fluctuations in superconducting nanocircuits

Recent work³⁴ suggested another kind of time-modulated small superconducting system. It is proposed that a mechanically driven superconducting single-electron transistor (SSET) may serve as a realization of the QKR. The system is based on a Cooper pair shuttle—a small superconducting island, periodically traveling between two macroscopic superconducting leads with the phases ϕ_L and ϕ_R , respectively [Fig. 9(a)]. Twice during each period, T , the shuttle meets one of the leads, experiencing a sudden Josephson coupling [cf. Fig. 9(b)]. The average coupling energy \bar{E}_J is assumed to be much larger than the charging energy E_c . If the two leads are far enough from each other, the island never couples to both leads simultaneously. If the switching time is short, the time-dependent Josephson coupling may be mimicked by delta pulses. Therefore, one may model the system with the following Hamiltonian:

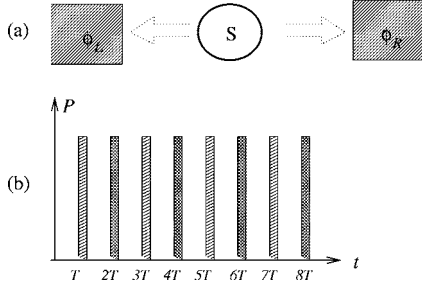


FIG. 9. A superconducting shuttle periodically travels between two superconducting leads with the phase ϕ_L and ϕ_R , respectively (a). At every other period $2T$, the shuttle experiences a sudden Josephson coupling with the left (right) lead. The power strength P is proportional to $\bar{E}_J T$ (b). At times which are odd multiples of T , the phase of the superconducting shuttle is shifted by $\Phi (\equiv \phi_R - \phi_L)$.

$$\hat{H} = -4E_c \frac{\partial^2}{\partial \theta^2} - \bar{E}_J T \sum_n [\cos \theta \delta(t - 2nT) + \cos(\theta + \Phi) \times \delta(t - (2n+1)T)]. \quad (108)$$

Here, θ is the relative phase of the superconducting island with respect to the right lead. Remarkably, the phase difference across the two superconducting leads, $\Phi \equiv \phi_R - \phi_L$ breaks the “time-reversal” symmetry, Eq. (8). The effective Planck constant and kicking strength remain the same as in Eq. (107). With the same rescaling as in Sec. VI B, Eq. (108) is rewritten as Eq. (90).

The classical-to-quantum crossover is reflected in the nonequilibrium charge fluctuations of the superconducting island. In the case of $\Phi=0$, the situation is the same as Sec. VI B. In the presence of a small phase bias across the two superconducting leads, i.e., $|\Phi| \lesssim \bar{\kappa}/K$, the charge fluctuations are described by Eq. (98). For larger phase bias $|\Phi| \gtrsim \bar{\kappa}/K$, the charge fluctuations are given by Eq. (102).

VII. WEAK-DYNAMICAL LOCALIZATION IN PRESENCE OF NOISE

Due to the quantum interference nature of the weak-dynamical localization, the effect may be strongly sensitive to noise. Indeed, noise effects are known to be of importance for the dynamical localization.^{32,53–55} So far, both experimental and theoretical studies have been primarily focused on $t_E \lesssim 1$. Below, we shall consider how an external noise affects classical-to-quantum crossover at time scales $t \gtrsim t_E$. To this end, we will employ the technique of Sec. IV to investigate a noise sensitivity of the weak-dynamical localization cooperon and Hikami box.

A. Phase noises

In proposed experiments involving small superconducting systems, the phase may fluctuate due to the influence of the dissipative measurement circuit. For the analytical treatment we focus on the particular kind of noises—the Gaussian phase noise. That is, the phase is assumed to fluctuate ran-

domly in time: $\theta_n \rightarrow \theta_n + \zeta_n$. Here, $\zeta_n \equiv \zeta_i$ is the noise that is assumed to be uncorrelated at different kicks $\langle \zeta_n \zeta_{n'} \rangle = 0$ for $n \neq n'$. At a given kick the random phase ζ is supposed to be drawn from some *periodic* distribution function $P(\zeta) = (2\pi)^{-1} \sum_m P_m e^{im\zeta}$. For simplicity, we shall assume that

$$P_m = e^{-\sigma_\varphi m^2}, \quad (109)$$

where σ_φ characterizes the strength of the noise.

1. Strong phase noise

The strong noise limit is characterized by $\sigma_\varphi \rightarrow \infty$, and thus $P(\zeta) = 1/2\pi$ being uniform distribution on $\zeta \in [0, 2\pi]$. We show first that the classical diffusion (without localization) is restored in this limit. The quantum density-density correlator satisfies [cf. Eq. (10)]

$$\begin{aligned} \mathcal{D}_\zeta(l_+, l_-; l'_+, l'_-) &= e^{i(l_+^2 - l_-^2)/2\bar{\kappa}} \delta_{l'_+, l'_-} \delta_{l_+, l_-} \\ &+ e^{i\omega} \sum_{l''_+, l''_-} \overline{\langle l_+ | \hat{U} | l''_+ \rangle \langle l_- | \hat{U} | l''_- \rangle^*} \\ &\times \mathcal{D}_\zeta(l''_+, l''_-; l'_+, l'_-; \omega), \end{aligned} \quad (110)$$

where the long bar stands for the average over the phase noise with respect to the uniform distribution, i.e.,

$$\begin{aligned} &\overline{\langle l_+ | \hat{U} | l''_+ \rangle \langle l_- | \hat{U} | l''_- \rangle^*} \\ &\equiv \int \frac{d\zeta}{2\pi} \frac{d\theta_+}{2\pi} \frac{d\theta_-}{2\pi} \exp \left\{ \frac{iK}{\bar{\kappa}} [\cos(\theta_+ + \zeta) - \cos(\theta_- + \zeta)] \right\} \\ &\times \exp \left[\frac{i(l_+^2 - l_-^2)}{2\bar{\kappa}} + \frac{i\theta_+}{\bar{\kappa}} (l_+ - l''_+) - \frac{i\theta_-}{\bar{\kappa}} (l_- - l''_-) \right] \\ &= \exp \left[\frac{i(l_+ + l_-)(l_+ - l_-)}{2\bar{\kappa}} \right] f(l_+ - l''_+) \delta_{l_+ - l''_+, l_- - l''_-}. \end{aligned} \quad (111)$$

In the last line, $f(l)$ is defined as

$$f(l) \equiv \int \frac{d\varphi}{2\pi} J_{2l} \left(\frac{2K}{\bar{\kappa}} \sin \frac{\bar{\kappa}\varphi}{2} \right). \quad (112)$$

With the definition $l \equiv (l_+ + l_-)/2$, $l' \equiv (l'_+ + l'_-)/2$, and $\Delta l \equiv l_+ - l_-$, the solution of Eq. (110) may be formally written as

$$\begin{aligned} \mathcal{D}_\zeta(l, l'; \Delta l) &= \exp \left[\frac{i\Delta l}{2\bar{\kappa}} \right] \delta_{l, l'} + \sum_{n=1}^{\infty} e^{i\omega n} \sum_{l_1, \dots, l_{n-1}} \exp \left[\frac{i\Delta l}{2\bar{\kappa}} \sum_{k=1}^n l_k \right] \\ &\times f(l - l_1) f(l_1 - l_2) \cdots f(l_{n-1} - l'), \end{aligned} \quad (113)$$

where $l_n \equiv l'$. As a result of the averaging over noises, \mathcal{D}_ζ has no ζ dependence. In the large K limit, we expect the solution to be independent of $(l+l')/2$. Thus, taking the average over $(l+l')/2$, one finds

$$\begin{aligned} \langle \mathcal{D}_\zeta(l, l') \rangle &= \delta_{l, l'} + \sum_{n=1}^{\infty} e^{i\omega n} \sum_{l_1, \dots, l_{n-1}} f(l - l_1) \\ &\quad \times f(l_1 - l_2) \cdots f(l_{n-1} - l'). \end{aligned} \quad (114)$$

Passing to Fourier representation, we find that it is nothing but the classical diffuson, Eq. (22). It is worth mentioning that in the strong noise limit the diffusion constant is *exactly* $K^2/4$. This is due to the fact that higher-order corrections¹¹ as well as quantum renormalization^{31,62} result from long-time correlation effects (cf. Appendix A). The latter is completely destroyed by the strong noise.

2. Weak phase noise limit

We turn now to a more interesting case, relevant to the context discussed here, i.e., $\sigma_\varphi \ll 1$, where the noise only slightly suppresses the weak-dynamical localization. For $\langle \zeta^2 \rangle \sim \sigma_\varphi \ll 1$, $\cos(\varphi + \zeta) \approx \cos \varphi - \zeta \sin \varphi$.

Let us concentrate on the effect of the noise on the cooperon. Upon every kicking, cooperon acquires an additional phase: $K(\zeta_t \cos \theta_+ - \zeta_{t'} \cos \theta_-)/\bar{k}$. Recall that t, t' are counted from the two opposite ends of the loop trajectory, and $t + t' \equiv T_t$, with T_t being the total duration of the loop. Since ζ_t and $\zeta_{t'}$ stand for noises at different moments, they are uncorrelated. Averaging the phase factor over them leads to the exponential suppression of every step of the cooperon ladder

$$\begin{aligned} &\left\langle \exp\left(\frac{iK\zeta_t}{\bar{k}} \cos \theta_+\right) \exp\left(-\frac{iK\zeta_{t'}}{\bar{k}} \cos \theta_-\right) \right\rangle_{\zeta_t, \zeta_{t'}} \\ &= e^{-K^2 \sigma_\varphi / 2\bar{k}^2} I_0^2\left(\frac{K^2 \sigma_\varphi}{4\bar{k}^2}\right). \end{aligned} \quad (115)$$

[$I_0(x)$ is the modified Bessel function.] This implies that the cooperon is suppressed as

$$C_0(t) \rightarrow C_0(t) e^{-t/t_\varphi}, \quad (116)$$

with the dephasing time defined as $t_\varphi = 2\bar{k}^2/(K^2 \sigma_\varphi)$. For $\sigma_\varphi \geq (\bar{k}/K)^2$, $t_\varphi \sim 1$, the cooperon mode is suppressed completely. It does not mean, however, that the classical diffusion is restored for such small σ_φ . Indeed, the higher-order loop corrections, that include the diffusons only (cf. Fig. 6) may still survive such level of the noise and lead to the dynamical localization. To verify if this is the case, one needs to study the effect of the weak noise on Hikami box.

Starting from Eqs. (49) and (56), we observe that $\delta\theta_1$ and θ' are independently shifted by the noise, i.e., $\delta\theta_1 \rightarrow \delta\theta'_1 \equiv \delta\theta_1 + \zeta_1$, $\theta' \rightarrow \theta' + \zeta_2$. As a result, instead of Eq. (55), \mathcal{X} is given by

$$\begin{aligned} \mathcal{X}(\delta l_1, \delta\theta_1; \delta l_2, \delta\theta_2) &\rightarrow \exp\left(\frac{iK\zeta \delta\theta'_1 \delta\theta_2}{\bar{k}} \sin \theta'\right) \\ &\quad \times \mathcal{X}(\delta l_1, \delta\theta'_1; \delta l_2, \delta\theta_2). \end{aligned} \quad (117)$$

Upon averaging over ζ , Eq. (117) leads to the exponential suppression of the minimal quantum wave packet (Hikami box) as

$$\exp\left[-\left(\frac{K\delta\theta'_1 \delta\theta_2}{2\bar{k}}\right)^2 \sigma_\varphi\right] \mathcal{X}(\delta l_1, \delta\theta'_1; \delta l_2, \delta\theta_2). \quad (118)$$

From here we see that the weak phase noises ($\sigma_\varphi \ll 1$) do not substantially affect the Hikami box. Indeed, the interaction vertex is significantly suppressed only at $\sigma_\varphi \sim 1$. This means that the effect of phase noises on Hikami box may be ignored compared to the dephasing of cooperon.

As a result, the intermediate intensity noise $(\bar{k}/K)^2 \ll \sigma_\varphi \ll 1$ acts, to a large extent, as a TRS breaking perturbation. It suppresses the cooperon corrections, leaving the diffuson ones (the simplest being the two-loop one, Fig. 6) intact.

Above, we find that the diffuson-cooperon coupling-minimal wave packet is suppressed by large enough phase noises. This picture is naturally expected to be applicable for higher-order interaction vertex also. The latter is essentially responsible for the onset of the weak-dynamical localization in diffuson-only diagrams. This picture may be considered to be the precursor of the restoration of diffusion for larger noises.

B. Amplitude noise

In cold atoms experiments, the optical pulse power may fluctuate with time and thus the series is not perfectly periodic. This then leads to the noise in the kicking amplitude, i.e., the stochastic parameter K is replaced by $K + \eta_n$, where $\eta_n = \eta_t$ is a random amplitude fluctuation. The effects on dynamical localization of such kind of noise have been under intensified experimental investigations.^{32,54,55} A central issue addressed is whether the dynamical localization is destroyed completely by the noise. We concentrate here on a weak noise limit.

To simplify analytical estimations below, let us assume that η_n is the white-noise Gaussian noise, namely $\langle \eta_n \eta_{n'} \rangle = \sigma_K \delta_{nn'}$. Here, σ_K characterizes the strength of the noise. Below, we consider the limiting case of $\sigma_K \ll 1$, where the amplitude noise only slightly suppresses the weak-dynamical localization.

For the diffuson the one-step quantum propagator acquires an additional phase as $\eta_t(\cos \theta_+ - \cos \theta_-)$. Here, θ_+, θ_- stand for the phases of retarded and advanced Green's functions at the kicks. Passing to the semiclassical limit, i.e., $|\theta_+ - \theta_-| \ll 1$ and averaging over the noise, we find that the diffuson is affected via renormalization of D_{cl} by a small correction, $\delta D_{cl} \sim \sigma_K \ll D_{cl}$. (A detailed study in this direction was presented in Ref. 3.) This correction is not responsible for the destruction of the dynamical localization. It is the effect of the noise on the cooperon and Hikami box that eventually may lead to the restoration of the classical diffusion.

In the case of the amplitude noise, the effect on the cooperon is fully analogous to the case of the phase noise, i.e., dephasing. Upon every kicking, the Cooperon acquires an additional phase: $(\eta_t \cos \theta_+ - \eta_{t'} \cos \theta_-)/\bar{k}$, with t, t' counted from the opposite ends, respectively, such that $t + t' \equiv T_t$, with T_t being the total duration of the loop. Upon averaging over

the independent noises η_t and $\eta_{t'}$, this phase factor leads to the exponential suppression of a single step of the cooperon as

$$\left\langle \exp\left(\frac{i\eta_t}{\hbar} \cos \theta_+\right) \exp\left(-\frac{i\eta_{t'}}{\hbar} \cos \theta_-\right) \right\rangle_{\eta_t, \eta_{t'}} = \exp\left[-\frac{\sigma_K}{2\hbar^2}\right] I_0^2\left(\frac{\sigma_K}{4\hbar^2}\right). \quad (119)$$

This implies that the cooperon is dephased as Eq. (116) with the dephasing time being $\tau_K = 2\hbar^2/\sigma_K$. For $\sigma_K \gtrsim \hbar^2$, $\tau_K \sim 1$, the cooperon mode is suppressed completely; thus, only higher-order terms (diffusons only) may be responsible for the dynamical localization. It remains open to estimate the noise amplitude that destroys diffuson-only weak dynamical localization.

C. Effects of finite dephasing time

We saw above that every realization of the QKR may involve various noises in realistic experimental environments. As a result, there exist various dephasing mechanisms. The effective dephasing rate is the sum over all dephasing rates, namely

$$\frac{1}{\tau_\varphi} = \sum_k \frac{1}{\tau_k}. \quad (120)$$

To simplify qualitative discussions, in this part we focus on effects arising from weak dephasing such that $4t_E \ll \tau_\varphi$. First, we show that the effective Ehrenfest time is shortened. In fact, the additional weak noises enhance the rate of angular deviation spread according to

$$\frac{d}{dt} \delta\theta^2(t) = 2\lambda \delta\theta^2(t) + \frac{1}{\tau_\varphi}. \quad (121)$$

Recall that the first term on the right-hand side results from the Lyapunov instability. The solution is easily found, i.e., $\delta\theta^2(t) = [\delta\theta_{1,2} + (2\lambda\tau_\varphi)^{-1}]e^{\lambda t} - (2\lambda\tau_\varphi)^{-1}$. Here, $\delta\theta_{1,2}$ are the initial angular deviation of diffuson and cooperon, respectively. At t^{D*} (or t^{C*}), $\delta\theta \sim 1$. The solution then gives

$$t^{D,C*} \approx \frac{1}{\lambda} \left| \ln \frac{1}{\sqrt{\delta\theta_{1,2}^2 + (2\lambda\tau_\varphi)^{-1}}} \right|. \quad (122)$$

Thus, the effective duration of a full travel through the Lyapunov region is found to be

$$\begin{aligned} t^{D*} + t^{C*} &= \frac{1}{\lambda} \left| \ln \frac{1}{\sqrt{(\delta\theta_1\delta\theta_2)^2 + (\delta\theta_1^2 + \delta\theta_2^2)(2\lambda\tau_\varphi)^{-1} + (2\lambda\tau_\varphi)^{-2}}} \right| \\ &\leq \frac{1}{\lambda} \left| \ln \frac{1}{|\delta\theta_1\delta\theta_2| + (2\lambda\tau_\varphi)^{-1}} \right| \\ &\sim \frac{2}{\lambda} \left| \ln \frac{1}{\sqrt{\frac{\hbar}{K} + (2\lambda\tau_\varphi)^{-1}}} \right| = 2t_E^*. \end{aligned} \quad (123)$$

The effective Ehrenfest time $t_E^* < t_E$. With t_E^* substituted into the renormalization factors \mathcal{W}_C and \mathcal{W}_D , and taking into account the dephasing of diffusive cooperon, the one-loop correction, Eq. (83), is modified as

$$\delta D(\omega) = -\frac{\hbar D_{cl}}{\pi} \mathcal{W}_D(2\omega) \mathcal{W}_C(2\omega) \int \frac{d\varphi}{-i\omega + D_{cl}\varphi^2 + \frac{1}{\tau_\varphi}}. \quad (124)$$

Taking the Fourier transform with respect to ω , one finds the momentum dispersion to be

$$\delta \langle l^2(t) \rangle = 2D_{cl}t - \frac{8\hbar\sqrt{D_{cl}}}{3\sqrt{\pi}} \theta(t - 4t_E^*)(t - 4t_E^*)^{3/2} e^{-(t-4t_E^*)/\tau_\varphi}. \quad (125)$$

Again, $\lambda_2 = 0$. According to Eq. (125) the quantum correction is suppressed at $t \gtrsim 4t_E^* + \tau_\varphi$.

One should keep in mind that in realistic experiments, like atom-optical ones the Hamiltonian of QKR, Eq. (1) may be an oversimplification. Therefore, some restriction on the validity of the present result will be imposed. For example, the cold atoms experiment involves collisions between the atoms, which leads to another dephasing mechanism. Let us estimate the corresponding collision dephasing time, τ_s . The two-particle scattering mean free path is known to be $l_s \approx 1/(na^2)$, where n is the atomic concentration and a is the s -wave scattering length. The corresponding dimensionless scattering time is $\tau_s = l_s/(Tv)$, where v is a typical atomic velocity that may be estimated as $v \approx \hbar k_L |l|/\hbar m \approx \hbar k_L \sqrt{D_{cl}\tau_s}/\hbar m$. This leads to the self-consistent estimate of the dimensionless dephasing time

$$\tau_s \approx (l_s k_L / K)^{2/3}. \quad (126)$$

Once again, to observe the classical-to-quantum crossover the inequality $4t_E \leq \tau_s$ should be valid. Another important factor leading to dephasing in atom-optical experiments is spontaneous emission.⁵⁶ It may quantitatively affect the dephasing rate according to Eq. (120). However, the qualitative result, i.e., Eq. (125), remains unchanged.

VIII. CONCLUSIONS

In this paper, we developed an analytical theory that systematically incorporates the Ehrenfest time, t_E , into the weak-dynamical localization. We map the loop expansion, central to the theory of the weak-dynamical localization, onto the interference of paths in the configuration space with a certain loop geometry. To propagate along such paths a time longer than $2mt_E$ ($m=2,3,\dots$) (where m is determined by a specific loop geometry) is needed. Thus, we establish that the onset of the dynamical localization is delayed by the multiples of $2t_E$. In particular, for QKR the delay is $4t_E$, while for systems with broken time-reversal symmetry it is $6t_E$. At shorter times, quantum corrections to the linear dispersion (classical diffusion) do exist. However, they lead to the renormalization of the frequency-independent diffusion

coefficient only. Thus, they are *not* responsible for the onset of the dynamical localization.

Our quantitative predictions are based on the loop expansion and are essentially perturbative. The perturbative corrections are responsible only for the early evolution of the dispersion function, i.e., the suppression of the classical diffusion. They are closely analogous to the weak Anderson localization in ballistic systems. At longer time $t \gtrsim t_L$, there is a long-standing conjecture claiming that the strong dynamical localization is expected to develop.¹³ This conjecture was supported by arguments based on supersymmetric diffusive σ model and in part has been proven rigorously by Bourgain and Jitomirskaya recently.⁵⁷ The present work may be considered as a further support for the similarity between the dynamical localization and Anderson localization.

The quantum dynamics of kicked rotor is very complicated. In particular, it exhibits the so-called quantum resonances at the rational values of $\hbar/4\pi$ (see Ref. 23 for a review). At such resonance points $\hbar/4\pi = p/q$, where p, q are coprime natural numbers, the long-time momentum dispersion grows quadratically with time. Our theory is certainly not applicable to this situation. However, the characteristic time scale for the quadratic growth to become dominant increases drastically with increasing q ;²³ thus, we still expect the present theory to be applicable for sufficiently large p and q . Unfortunately, we are not able to further give the quantitative restriction.

The result presented in this work may be extended to more general quantum driven systems. The essential requirements imposed on the dynamics of an underlying classical system are: (i) area preserving; and (ii) the existence of classical stochastic diffusion (subject to a certain symmetry). Provided (i) and (ii) are satisfied, we expect the functional form of the weak localization corrections to be the same as derived above. The specific nature of the chaotic motion enters through the classical quantities such as diffusion coefficient, Lyapunov exponent, and its fluctuations. These three purely classical objects, in general, may be found (say numerically) and substituted into the derived expressions for the localization corrections. In particular, the present result may be relevant to studies of the energy growth near quantum resonance in ultracold atomic gases.⁵⁸ It was shown^{58,59} that the quantum dynamics with $\hbar/4\pi$ close to a rational number may be mapped back onto the *classical* standard map. In this case a small deviation of $\hbar/4\pi$ from the rational number plays a role of the effective Planck's constant. Our formalism may prove to be useful to study localization in the proximity to a rational value situation.

The analytical treatment developed here may be applicable to other chaotic systems. In particular, there exist systems where the weak localization is found while the strong localization is not observed. In general, the underlying phase space of such systems is not one-dimensional or quasi-one-dimensional. Along these directions a refined diagrammatic technique has been employed recently by two of us to show the deterministic weak localization for periodic Lorentz gases with a finite horizon.⁶⁰ The analytical tool developed in the present work may be also adapted to explore problems where the weak localization corrections can be found but

traditionally are described by the random matrix theory, such as the level statistics in chaotic quantum billiards.^{44,61}

Technically, the most important part of this work is the derivation of the one-loop vertex (Hikami box) *without* introduction of a regularization. This allows us to analyze accurately the minimal quantum wave packet. As a result, the Ehrenfest time is quantitatively defined (with the logarithmic accuracy) as the time needed to expand an initial minimal wave packet up to a macroscopic size.^{21,22} Alternatively, the minimal wave packet may be analyzed within the Moyal formalism.^{37,63} A study along these lines has been reported recently in the context of ballistic supersymmetric σ model.³⁰ This supports the conjecture of Ref. 27 that the Ehrenfest time should not depend on the regularization, since the latter is only intended to mimic the effect of quantum diffraction. Indeed, in accord with Ref. 27, our current results may be fully reproduced by introducing a proper regularization³⁷ to the supersymmetric σ model developed for QKR.¹⁹

The quantitative predictions made for the t_E -dependent classical-to-quantum crossover in QKR may be suitable for experimental verifications in various contexts. In particular, already-existing experiments on the dynamical localization in the energy growth of ultracold atomic gases have greatly contributed to understanding of this crossover. Our quantitative predictions are expected to be accurate in the asymptotic regime $\hbar < 1 < K$. For their quantitative verification, it is thus highly desirable to decrease \hbar down to 0.1–1. We also pointed out that some periodically driven mesoscopic superconducting structures may be suitable for realizations of the QKR. The dynamical localization and classical-to-quantum crossover in these systems are observable by monitoring charge fluctuations of the superconducting island. It is important to mention that all realistic experiments introduce noise and thus a finite dephasing time τ_ϕ . We have shown here that for an observation of the t_E -dependent crossover, the condition $4t_E \lesssim \tau_\phi$ must be satisfied.

ACKNOWLEDGMENTS

We have greatly benefited from discussions with A. Altland, D. Basko, S. Fishman, V. E. Kravtsov, J. Liu, and C. Zhang. We thank L. Glazman for pointing out Ref. 35 to us. We are grateful to Abdus Salam International Center for Theoretical Physics, where part of this work was done, for its hospitality. C. T. and A. L. are supported by NSF under Grants No. DMR-0120702, DMR-0439026, and partly by PHY-9907949. A. K. acknowledges support from A. P. Sloan foundation and the NSF Grant No. DMR-0405212.

APPENDIX A: FINITE TIME-CORRELATION EFFECTS ON THE SELF-ENERGY

In this appendix we study the higher-order time correlation effects, starting from the exact quantum density-density correlator, Eq. (12). In particular, we clarify that in the semiclassical limit, the higher-order corrections, namely Eq. (24), (see Ref. 11) to the diffusion constant, i.e., $K^2/4$ are found.

For an arbitrary $\tau_c > 1$, Eq. (19) is replaced by

$$\mathcal{D}_0(l, l') = \delta_{l, l'} + \sum_{l''} \Sigma(l, l'') \mathcal{D}_0(l'', l'). \quad (\text{A1})$$

Here, the self-energy, $\Sigma(l, l'')$, is given by

$$\begin{aligned} \Sigma(l, l'') &= \sum_{n=1}^{\tau_c} e^{i\omega n} \langle l | \hat{U}^n | l'' \rangle \langle l | \hat{U}^n | l'' \rangle^* \\ &= e^{i\omega} U_{l, l''} U_{l, l''}^* \\ &\quad \times \sum_{n=2}^{\tau_c} e^{i\omega n} \sum_{l_1+, l_1-} \dots \sum_{l_{(n-1)+}, l_{(n-1)-}} \\ &\quad \times \prod_{k=1}^{n-1} U_{l_{k+}, l_{(k+)+}} U_{l_{k-}, l_{(k+)-}}^*. \end{aligned} \quad (\text{A2})$$

Note that $l_0 = l'_0 \equiv l$, $l_n = l'_n \equiv l''$, and $l_k \neq l'_k$ for $0 < k < n$. Here, in order to simplify the notation we denote the matrix elements $\langle l_{k+} | \hat{U} | l_{(k+)+} \rangle$ as $U_{l_{k+}, l_{(k+)+}}$, and similarly for their complex conjugates. These matrix elements may be written explicitly as

$$\begin{aligned} U_{l_{k+}, l_{(k+)+}} &= \int \frac{d\theta_{(k+)+}}{2\pi} \exp \left[\frac{i l_{(k+)+}^2}{2\hbar} + \frac{iK}{\hbar} \cos \theta_{(k+)+} \right. \\ &\quad \left. - \frac{i}{\hbar} (l_{k+} - l_{(k+)+}) \theta_{(k+)+} \right], \\ U_{l_{k-}, l_{(k+)-}}^* &= \int \frac{d\theta_{(k+)-}}{2\pi} \exp \left[-\frac{i l_{(k+)-}^2}{2\hbar} - \frac{iK}{\hbar} \cos \theta_{(k+)-} \right. \\ &\quad \left. + \frac{i}{\hbar} (l_{k-} - l_{(k+)-}) \theta_{(k+)-} \right]. \end{aligned} \quad (\text{A3})$$

To proceed further, we introduce the following quantities:

$$m_k = (l_{k+} - l_{k-})/\hbar, q_k = (\theta_{k+} - \theta_{k-})/\hbar. \quad (\text{A4})$$

Then, with the substitution of Eq. (A3) we rewrite $U_{l_{k+}, l_{(k+)+}} U_{l_{k-}, l_{(k+)-}}^*$ as

$$\begin{aligned} &U_{l_{k+}, l_{(k+)+}} U_{l_{k-}, l_{(k+)-}}^* \\ &= \int \int \frac{d\theta_{(k+)+}}{2\pi} \frac{d\theta_{(k+)-}}{2\pi} \exp \left\{ im_{k+1} \frac{l_{(k+)+} + l_{(k+)-}}{2} - \frac{2iK}{\hbar} \right. \\ &\quad \times \sin \frac{\hbar q_{k+1}}{2} \sin \frac{\theta_{(k+)+} + \theta_{(k+)-}}{2} - iq_{k+1} \\ &\quad \times \left[\frac{l_{k+} + l_{k-}}{2} - \frac{l_{(k+)+} + l_{(k+)-}}{2} \right] + i(m_k \\ &\quad \left. - m_{k+1}) \frac{\theta_{(k+)+} + \theta_{(k+)-}}{2} \right\}. \end{aligned} \quad (\text{A5})$$

Furthermore, we insert the Fourier transform

$$\exp \left[\frac{2iK}{\hbar} \sin \theta \sin \frac{\hbar q}{2} \right] = \sum_n J_n \operatorname{sgn} q \left(\frac{2K}{\hbar} \sin \frac{\hbar q}{2} \right) e^{in\theta} \quad (\text{A6})$$

into it with sgn denoting the sign of q . Then, Eq. (A5) is substituted into Eq. (A2). With the sum with respect to $(l_{k+} + l_{k-})/2$ ($k=0, 1, 2, \dots$) and the integral with respect to $(\theta_{k+} + \theta_{k-})/2$ performed, eventually Eq. (A2) is reduced to

$$\begin{aligned} \Sigma(l, l'') &= e^{i\omega} J_0 \left(\frac{2K}{\hbar} \sin \hbar q_0 \right) \\ &\quad + \sum_{r=2}^{\tau_c} e^{i\omega r} \sum_{n_1, n_2, \dots, n_r} \sum_{m_1, m_2, \dots, m_{r-1}} \sum_{q_0, q_1, \dots, q_{r-1}} \prod_{k=1}^r \\ &\quad \times J_{n_k \operatorname{sgn} q_{k-1}} \left(\frac{2K}{\hbar} \left| \sin \frac{\hbar q_{k-1}}{2} \right| \right) \\ &\quad \times \delta_{q_k - q_{k-1} - m_k} \delta_{m_k - m_{k-1} - n_k \operatorname{sgn} q_{k-1}}. \end{aligned} \quad (\text{A7})$$

Shortly, we will see that the following relations, implied by the two Kroneck's symbols:

$$q_k = q_{k-1} - m_k, \quad (\text{A8})$$

and

$$m_k = m_{k-1} - n_k \operatorname{sgn} q_{k-1}, \quad (\text{A9})$$

are essential for the derivation of higher-order corrections to the diffusion constant.¹¹ It is in order to emphasize that they are exact even at the quantum-mechanical level, although originally found in the classical context.¹¹

Note that above $m_0 = m_n = 0$. So far, the discussions above are formally accurate. We assume now that the correlator, $\mathcal{D}_0(l, l')$, does not depend on the center of mass, namely $\mathcal{D}_0(l, l') = \mathcal{D}_0(l - l')$. This is supplemented by performing Fourier transformation for $\mathcal{D}_0(l - l')$

$$\mathcal{D}_0(l - l') = \int \frac{d\varphi}{2\pi} \mathcal{D}_0(\varphi) e^{i\varphi(l - l')}, \quad (\text{A10})$$

and imposing the boundary condition as (resulting from finite τ_c)¹¹

$$q_0 = q_{r-1} = \varphi \rightarrow 0, \quad (\text{A11})$$

with φ denoting the Fourier component. Then, Fourier transforming $\Sigma(l-l')$ leads to

$$\begin{aligned} \Sigma(\varphi) &= e^{i\omega} J_0 \left(\frac{2K}{\hbar} \sin \frac{\hbar\varphi}{2} \right) \\ &+ \sum_{r=2}^{\tau_c} e^{i\omega r} \sum_{n_1 \neq 0} \sum_{n_2, \dots, n_r} \sum_{m_1, m_2, \dots, m_{r-1}} \sum_{q_1, \dots, q_{r-2}} \prod_{k=1}^r \\ &\times J_{n_1} \left(\frac{2K}{\hbar} \sin \frac{\hbar\varphi}{2} \right) J_{n_r} \left(\frac{2K}{\hbar} \sin \frac{\hbar\varphi}{2} \right) \\ &\times J_{n_k \operatorname{sgn} q_{k-1}} \left(\frac{2K}{\hbar} \left| \sin \frac{\hbar q_{k-1}}{2} \right| \right). \end{aligned} \quad (\text{A12})$$

Note that above we suppressed the two Kroneck's symbols to simplify the expression. One should keep in mind that the sum over m 's, q 's, and n 's is restricted by the two "motion" equations, i.e., Eq. (A8) and (A9).

Let us make the semiclassical approximation, i.e., $|\hbar q_k| \ll 1$ in Eq. (A12) and focus on the limit $K\varphi \ll 1$. The first term in the self-energy leads to the diffusion constant as $K^2/4$, as discussed in Sec. III B. The second term gives higher-order oscillatory corrections. In fact, up to $(K\varphi)^2$, the sum is contributed by a particular series of (q_k, m_k) ($k=0, 1, 2, \dots$) (so-called Fourier paths)¹¹ as $(\varphi, 0) \rightarrow \pm(0, 1) \cdots \pm(1, -1) \rightarrow (\varphi, 0)$. Here, \cdots is shorthand for product of Bessel functions, which is an expansion in powers of $K^{-1/2}$. Since for $K\varphi \ll 1$, $J_n(K\varphi) \sim (K\varphi)^n$, therefore, $n_{1,r} = \pm 1$ is the only contribution to the order $(K\varphi)^2$. This then leads to $\Sigma(\varphi)$ as¹¹

$$\begin{aligned} \Sigma(\varphi) &= e^{i\omega} J_0(K\varphi) \\ &+ \sum_{r=2}^{\tau_c} e^{i\omega r} \sum_{n_1, n_r = \pm 1} \sum_{n_2, \dots, n_{r-1}} \sum_{m_1, m_2, \dots, m_{r-1}} \sum_{q_1, \dots, q_{r-2}} \prod_{k=1}^r \\ &\times J_{n_1}(K\varphi) J_{n_r}(K\varphi) J_{n_k \operatorname{sgn} q_{k-1}}(2K|q_{k-1}|). \end{aligned} \quad (\text{A13})$$

In the limit $\omega\tau_c \ll 1$, $K\varphi \ll 1$, one recovers the diffuson Eq. (23) with the diffusion constant given by Eq. (24) up to $\mathcal{O}(1)$ (for $K \gg 1$).¹¹

Proceeding along this line, we may reproduce Shepelansky's result for the quantum diffusion constant of an early evolution (i.e., $\tau_c \leq 4$).^{31,62} The basic observation is that if the number of kicks is less than 4, then $q_k=1$. Based on Eq. (A12), this implies that Eq. (24) still holds except that K is replaced by $2K \sin(\hbar/2)/\hbar$.

APPENDIX B: TWO RELATIONS RESULTING FROM TRS

In this appendix we show two exact relations reflecting TRS. In the first, for any $n > 0$

$$\mathcal{D}_0(l, \theta; l', \theta'; n) = \mathcal{D}_0(l', -\theta'; l, -\theta; n). \quad (\text{B1})$$

Proof. Use the mathematical deduction. For $n=1$

$$\begin{aligned} \mathcal{D}_0(l, \theta; l', \theta'; 1) &= \vec{P} \delta(l-l') \delta(\theta - \theta' - l') \\ &= \delta[l - K \sin(\theta - l) - l'] \delta(\theta - l - \theta' - l'). \end{aligned} \quad (\text{B2})$$

On the other hand

$$\begin{aligned} \mathcal{D}_0(l', -\theta'; l, -\theta; 1) &= \vec{P} \delta(l' - l) \delta(-\theta' + \theta - l) \\ &= \delta[l' + K \sin(\theta' + l') - l] \\ &\quad \times \delta(-\theta' - l' + \theta - l) \\ &= \delta[l' + K \sin(\theta - l) - l] \\ &\quad \times \delta(\theta - l - \theta' - l'). \end{aligned} \quad (\text{B3})$$

Comparing the last two lines of Eqs. (B2) and (B3), we immediately see that Eq. (B1) holds for $n=1$. Next, we assume that Eq. (B1) holds for arbitrary $n=k > 1$. Then, for $n=k+1$, we obtain

$$\begin{aligned} \mathcal{D}_0(l', -\theta'; l, -\theta; k+1) &= \vec{P} \mathcal{D}_0(l', -\theta'; l, -\theta; k) \\ &= \vec{P} \mathcal{D}_0(l, \theta; l', \theta'; k) \\ &\equiv \mathcal{D}_0(l, \theta; l', \theta'; k+1). \end{aligned} \quad (\text{B4})$$

Thus, Eq. (B1) also holds for $n=k+1$. Q.E.D.

Now, we turn to show the other relation. That is, if

$$f(l, \theta; l', \theta') = f(l', -\theta'; l, -\theta), \quad (\text{B5})$$

then

$$\vec{P} f(l, \theta; l', \theta') = f(l, \theta; l', \theta') \vec{P}_T. \quad (\text{B6})$$

Proof

$$\begin{aligned} f(l, \theta; l', \theta') \vec{P}_T &= f(l, \theta; l' + K \sin(\theta' + l'), \theta' + l') \\ &= f[l' + K \sin(\theta' + l'), -(\theta' + l'); l, -\theta] \\ &= \vec{P} f(l', -\theta'; l, -\theta) \\ &= \vec{P} f(l, \theta; l', \theta'), \end{aligned} \quad (\text{B7})$$

where we used the definition, Eq. (31), in the second line, Eq. (B5) in the third and fifth lines, and the definition, Eq. (18), in the fourth line. Q.E.D.

APPENDIX C: DERIVATION OF RENORMALIZATION FACTOR OF DIFFUSIVE COOPERON

In this appendix, we derive the renormalization factor, Eq. (38), describing modification of the diffusive cooperon due to the propagation through the Lyapunov region. We first analyze the asymptotic instability of a generic chaotic trajectory.

1. Asymptotic instability

By varying the equations of motion of the classical kicked rotor

$$\frac{d\theta}{dt} = l,$$

$$\frac{dl}{dt} = K \sin \theta \sum_n \delta(t-n), \quad (\text{C1})$$

and defining the variables $z \equiv \ln|\delta\theta|$, $\alpha \equiv \delta l / \delta\theta$, we obtain

$$\frac{dz}{dt} = \alpha,$$

$$\frac{d\alpha}{dt} + \alpha^2 = K \cos \theta \sum_n \delta(t-n), \quad (\text{C2})$$

which describes the evolution of separation of two nearby trajectories along a reference trajectory, initiated from (l_0, θ_0) . From Eq. (C2) we see that α is a fast-changing variable. That is, the dynamics of α introduces some classical time scale, beyond which the slow-changing variable— z is independent of initial α . Let us further introduce the variables: α_n —denoting α right after the n th kicking, and z_n —denoting z at the n th kicking. Equivalently, we rewrite Eq. (C2) as

$$z_{n+1} - z_n = \ln(1 + \alpha_n),$$

$$\alpha|_{n+1} = \frac{1}{\alpha^{-1}|_n + 1} + K \cos \theta_{n+1}. \quad (\text{C3})$$

For $n \gg 1$, $\langle z_n \rangle = \lambda n$, $\langle (z_n - \lambda n)^2 \rangle = 2\lambda_2 n$. Thus, the Lyapunov exponent λ and its fluctuation λ_2 , characterizing the long-time instability, are defined as

$$\lambda = \lim_{n \rightarrow \infty} \lambda(n), \quad \lambda_2 = \lim_{n \rightarrow \infty} \lambda_2(n),$$

$$\lambda(n) = \frac{1}{n} \sum_{n'=0}^{n-1} \ln(1 + \alpha|_{n'}),$$

$$\lambda_2(n) = \frac{1}{n} \left[\sum_{n'=0}^{n-1} \ln(1 + \alpha|_{n'}) - n\lambda \right]^2, \quad (\text{C4})$$

respectively. Note that at finite times, they are trajectory dependent. In the limit $n \rightarrow \infty$, the time average is expected to be equivalent to the average over α , as well as the initial conditions located in the stochastic region.

The estimation of λ and λ_2 in the limit $K \gg 1$ may be made as follows based on the simple analysis above:

$$\lambda \equiv \langle \ln|K \cos \theta| \rangle = \ln(K/2);$$

$$\lambda_2 \equiv \langle \ln^2|K \cos \theta| \rangle - \lambda^2 = \zeta(3) - \ln^2 2 \approx 0.82, \quad (\text{C5})$$

where the angular brackets imply uniform averaging over the angle.

2. Renormalization factor

According to the definition of n_c , Eq. (35) it is the kick number when $z \approx 0$ with the logarithmic accuracy. That is

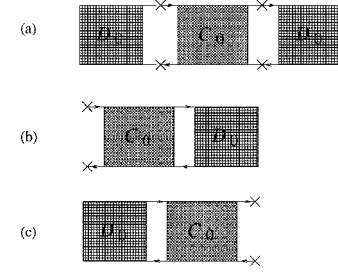


FIG. 10. Diagrams that lead to the interaction vertex with the particle conservation law respected: (a) $\delta\hat{D}_1$; (b) $\delta\hat{D}_2$; and (c) $\delta\hat{D}_3$.

$$0 = z_0 + \sum_{j=0}^{n_c-1} \ln(1 + \alpha|_j), \quad (\text{C6})$$

equivalently

$$n_c = -\frac{1}{\lambda(n_c)} \left\{ z_0 + \sum_{j=0}^{n_c-1} [\ln(1 + \alpha|_j) - \lambda(n_c)] \right\}. \quad (\text{C7})$$

Here, z_0 is some function of the initial deviations $(\delta l_0, \delta\theta_0)$. The exact form of z_0 is unessential. For an estimate, we notice that in the limit $K \gg 1$ the evolution of $\delta\theta_n$ may be approximated as $(\delta\theta_0 + \delta l_0 / K \cos \theta_0) \prod_{k=0}^{n-1} K \cos \theta_k$. Therefore

$$z_0 = \ln|\delta\theta_0 + \delta l_0 / K \cos \theta_0| \approx \ln \sqrt{\delta\theta_0^2 + \delta l_0^2 / K^2}. \quad (\text{C8})$$

Substituting Eq. (C7) into $\exp(2i\omega n_c)$, we obtain

$$e^{2i\omega n_c} = \exp \left[-\frac{2i\omega z_0}{\lambda(n_c)} \right]$$

$$\times \exp \left\{ -\frac{2i\omega}{\lambda(n_c)} \sum_{j=0}^{n_c-1} [\ln(1 + \alpha|_j) - \lambda(n_c)] \right\}$$

$$\approx \exp \left[-\frac{2i\omega z_0}{\lambda(n_c)} \right] \exp \left[-\frac{2\omega^2 \lambda_2(n_c) z_0}{\lambda^2(n_c)} \right], \quad (\text{C9})$$

where in the second line we use the fact that $\omega \lambda_2(n_c) n_c / \lambda^2(n_c) \ll 1$. In the limit $n_c \gg 1$, $\lambda(n_c) \rightarrow \lambda$, $\lambda_2(n_c) \rightarrow \lambda_2$. Moreover, from Eq. (C7) we see that $n_c \rightarrow t^C \equiv -z_0 / \lambda$. Thus, Eq. (C9) is reduced to Eq. (38).

APPENDIX D: THE EXACT INTERACTION VERTEX

In this appendix we discuss the exact interaction vertex appearing in the one-loop calculation. The general diagram, sketched in Fig. 5, may be categorized into three classes, Figs. 10(a)–10(c). In order to make the formula compact, let us write them in the operator representation as

$$\delta\hat{D}_1 = (e^{i\omega\hat{P}\hat{D}})\hat{C}(e^{i\omega\hat{P}\hat{D}}), \quad (\text{D1})$$

$$\delta\hat{D}_2 = \hat{P}_V \hat{C} \hat{D}, \quad (\text{D2})$$

$$\delta\hat{D}_3 = \hat{D} \hat{C} \hat{P}_V. \quad (\text{D3})$$

We then insert the identity

$$e^{i\omega\hat{P}} \equiv 1 + (e^{i\omega\hat{P}} - 1), \quad (\text{D4})$$

into Eq. (D1) and rewrite $\hat{\delta D}_1$ as

$$\hat{\delta D}_1 \equiv \hat{D}\hat{C}\hat{D} + \hat{\delta D}'_1 + \hat{\delta D}_4, \quad (\text{D5})$$

with

$$\hat{\delta D}'_1 = [(e^{i\omega\hat{P}} - 1)\hat{D}]\hat{C}\hat{D} + \hat{D}\hat{C}[(e^{i\omega\hat{P}} - 1)\hat{D}],$$

$$\hat{\delta D}_4 = [(e^{i\omega\hat{P}} - 1)\hat{D}]\hat{C}[(e^{i\omega\hat{P}} - 1)\hat{D}]. \quad (\text{D6})$$

For the first term in Eq. (D5), it was proved by Altland¹⁸ that it vanishes in the quantum limit, i.e., $\hbar \gg 1$. In the next section, we show that this term is indeed pure classical, and does not contribute to the quantum interference correction. We also show that the loop expansion does not violate the particle conservation law. As a result, the form of the interaction vertex implies that the quantum corrections may be reduced to the renormalization of the diffusion coefficient.

1. Semiclassical analysis on $\hat{D}\hat{C}\hat{D}$

Under appropriate approximation, it was proved that $\hat{D}\hat{C}\hat{D}$ is included in the *classical diffusive* propagator.¹⁸ Thus, it does not violate the diffusion equation. Since we are interested in the dynamics involving Ehrenfest time, the diffusive propagator cannot serve as a starting point of the formalism developed here. A natural question is whether this conclusion may still be applicable. Although it remains a challenge to prove at the accurate level, here we present a physical interpretation. We conclude that this term is pure classical, included in the exact classical propagator solution of the FPR equation.

For quantitative discussions below, let us denote the angular momenta and angles, appearing in the retarded and advanced propagator lines of cooperon as $l_{1\pm}, l_{2\pm}, \dots, l_{n\pm}$ and $\theta_{1\pm}, \theta_{2\pm}, \dots, \theta_{(n-1)\pm}$ following the forward time direction of the retarded line (see Fig. 5 for notations). Counting from the left-most side of the Cooperon and following the backward time direction of the retarded line, we denote those as $l_{0\pm}, l_{-1\pm}, l_{-2\pm}, \dots$, and $\theta_{0\pm}, \theta_{-1\pm}, \theta_{-2\pm}, \dots$. Semiclassically, only the constraint below

$$|\theta_{1+} + \theta_{(n-1)-}| \sim |\theta_{2+} + \theta_{(n-2)-}| \cdots |\theta_{(n-1)+} + \theta_{1-}| \leq \hbar, \quad (\text{D7})$$

is imposed.

According to the exact Eq. (A8), at the boundary of cooperon and (left) diffuson

$$(\theta_{1+} - \theta_{1-}) = (\theta_{0+} - \theta_{0-}) - (l_{1+} - \theta_{1-}). \quad (\text{D8})$$

On the other hand, Eq. (D7) does not impose any constraints on $\theta_{1+} - \theta_{1-}$. If it is order \hbar , the usual Wigner transform may be performed [see Eq. (14)]. That is to say, the left-most kicks of the cooperon may be incorporated into the left diffuson.

This discussion remains applicable for all successive pairs of kicks of the cooperon, until we meet some $k > 1$, where

$\theta_{k+} - \theta_{k-} \sim 1$ —a typical feature of the cooperon. This is equivalent to the validity of Eq. (D8) with the right-hand side of order 1. In fact, $(\theta_{0+} - \theta_{0-})$ and $(l_{1+} - \theta_{1-})$ develop from the left (classical) diffuson following Eqs. (A8) and (A9). In the diffuson side, $(\theta_{k+} - \theta_{k-}) (k = -1, -2, \dots), (l_{k+} - l_{k-}) (k = 0, -1, -2, \dots)$ are of order \hbar . Moreover, any evolution can last at most finite classical correlation time τ_c . Thus, $(\theta_{1+} - \theta_{1-})$ must be of order \hbar . Thus, Eq. (D8) cannot be satisfied if $(\theta_{1+} - \theta_{1-}) \sim \mathcal{O}(1)$.

Thus, we may conclude that $\hat{D}\hat{C}\hat{D}$ is pure classical. It characterizes the classical probability of trajectories with a peculiar feature. Since $|\theta_{1-} + \theta_{n+}| \leq \hbar \ll 1$, $\theta_{1+} \sim \theta_{1-} \sim -\theta_{n+}$, the trajectory switches its angle to the direction (almost) opposite to the initial.

2. A cancellation mechanism

Having the general expression Eq. (53) at hand, we turn to show that $\hat{\delta D}'_1, \hat{\delta D}_2, \hat{\delta D}_3$ cancel each other at the semiclassical level, namely

$$\hat{\delta D}'_1 + \hat{\delta D}_2 + \hat{\delta D}_3 \equiv 0. \quad (\text{D9})$$

Indeed, employing identity, Eq. (B6), we obtain

$$\begin{aligned} \hat{\delta D}'_1(l, \theta; l', \theta') &= \hat{\mathcal{V}} \left\{ \mathcal{D}_0 \left(l, \theta; l'' + \frac{\delta l_2}{2}, \theta' + \frac{\delta \theta_1}{2} \right) \right. \\ &\quad \times [(e^{i\omega\vec{P}_T} - 1) + (e^{i\omega\vec{P}} - 1)] \\ &\quad \left. \times \mathcal{D}_0 \left(l'' - \frac{\delta l_2}{2}, -\theta' + \frac{\delta \theta_1}{2}; l', \theta' \right) \right\}, \end{aligned} \quad (\text{D10})$$

$$\begin{aligned} \hat{\delta D}_2(l, \theta; l', \theta') &= \hat{\mathcal{V}} \left\{ 2\pi\hbar \delta \left[l - \left(l'' + \frac{\delta l_2}{2} \right) \right] \delta \left[\theta - \left(\theta' + \frac{\delta \theta_1}{2} \right) \right] \right. \\ &\quad \left. - l \right\} \times \mathcal{D}_0 \left(l'' - \frac{\delta l_2}{2}, -\theta' + \frac{\delta \theta_1}{2}; l', \theta' \right), \end{aligned} \quad (\text{D11})$$

and

$$\begin{aligned} \hat{\delta D}_3(l, \theta; l', \theta') &= \hat{\mathcal{V}} \left[\mathcal{D}_0 \left(l, \theta; l'' + \frac{\delta l_2}{2}, \theta' + \frac{\delta \theta_1}{2} \right) \right. \\ &\quad \times 2\pi\hbar \delta \left(l'' - \frac{\delta l_2}{2} - l' \right) \\ &\quad \left. \times \delta \left(-\theta' + \frac{\delta \theta_1}{2} - \theta' - l'' - \frac{\delta l_2}{2} \right) \right]. \end{aligned} \quad (\text{D12})$$

Since \mathcal{D}_0 is the solution of the FPR equation, i.e., Eq. (17), these three terms cancel each other. Therefore, we find that only $\hat{\delta D}_4$ leads to the nonvanishing one-loop correction to the classical density-density correlator.

APPENDIX E: ALEINER-LARKIN REGULARIZATION IN KICKED ROTOR

It is easy to see that in the classical limit $\hbar \rightarrow 0$, the functional form of $\delta\mathcal{D}'_1$ and $\delta\mathcal{D}_{2,3}$, i.e., Eqs. (D10)–(D12) are identical to what have been found for classical Lorentz gas (leaving the feature of standard map aside). These terms cancel each other, leading to the absence of the weak-localization correction. Remarkably, this cancellation still holds, even if the initial minimal wave packet is taken into account. On the other hand, the weak-localization correction *does* exist, given by the exact vertex $\delta\mathcal{D}_4$, which is absent in the expansion of ballistic supersymmetric σ model (without a regularizer). In this way, one may wonder whether an appropriate regularization may lead to a physical description of weak localization in semiclassical chaotic systems. This, indeed, was developed by Aleiner and Larkin for ballistic electronic problems.^{27,61} However, an important issue remains open whether and to what extent the physical results depend on the regularizer, rather than on the intrinsic quantum nature of the problem. The exact interaction vertex may serve as a testing ground of this regularization.

In fact, the regularization introduced in Refs. 27 and 61 is also applicable for QKR. To this end we try to mimic the “Born impurity” by modifying the (quantum) free rotation operator $\hat{\mathcal{P}}_V$ in the following way:

$$\hat{\mathcal{P}}_V \rightarrow \hat{\mathcal{P}}_V \exp\left(\frac{i\delta\hat{\mathcal{S}}}{\hbar}\right). \quad (\text{E1})$$

Here, $\delta\hat{\mathcal{S}}$ is some stationary random perturbation that commutes with $\hat{\mathcal{P}}_V$, i.e., $[\delta\hat{\mathcal{S}}, \hat{\mathcal{P}}_V] = 0$. Moreover, we assume that it is short-ranged correlated in the angular momentum space

$$\langle \delta_l \delta_{S_l} \delta_{l'} \delta_{S_{l'}} \rangle = \frac{2}{\tau_q} \delta_{l,l'}. \quad (\text{E2})$$

In the classical limit, this additional stationary random perturbations leads to the modification of the standard mapping in the following way:

$$l_{n+1} = l_n + K \sin \theta_n,$$

$$\theta_{n+1} = \theta_n + l_{n+1} + \partial_{l_{n+1}} \delta S_{l_{n+1}}. \quad (\text{E3})$$

Then, following the same procedure as in Ref. 27, we find the one-loop correction to the density-density correlator to be

$$\begin{aligned} \delta\mathcal{D}(l, \theta; l', \theta') &= \frac{2}{\tau_q} \int \frac{dl_1 d\theta_1}{2\pi\hbar} \mathcal{C}(l_1, \theta_1; l_1, -\theta_1) \\ &\times \left[\frac{\partial}{\partial\theta_1} e^{i\omega\vec{P}} \mathcal{D}(l, \theta; l_1, \theta_1) \right] \\ &\times \left[\frac{\partial}{\partial\theta_1} e^{i\omega\vec{P}} \mathcal{D}(l_1, -\theta_1; l', \theta') \right], \quad (\text{E4}) \end{aligned}$$

with the regularized diffuson \mathcal{D} and the cooperon \mathcal{C} satisfying the following equation:

$$\begin{aligned} \left[1 - \left(1 + \frac{1}{\tau_q} \frac{\partial^2}{\partial\theta^2} \right) e^{i\omega\vec{P}} \right] \begin{Bmatrix} \mathcal{D}(l, \theta; l', \theta') \\ \mathcal{C}(l, \theta; l', \theta') \end{Bmatrix} \\ = 2\pi\hbar \delta(l-l') \delta(\theta-\theta'). \quad (\text{E5}) \end{aligned}$$

Equations (E4) and (E5) are fully analogous to those found for ballistic electronic systems. In Eq. (E5), the regularizer of the FRP equation mimics the spread of the minimal wave packet arising from *intrinsic* quantum diffractions. Originally, it was expected²⁷ that the only physical effect arising from this regularizer is to determine the Ehrenfest time since it smears the sharp classical propagator. Indeed, one may further follow the procedure of Ref. 27 to calculate the weak-localization correction to the diffusion constant. As a result, the functional form of Eq. (83) is reproduced with t_E acquiring explicit τ_q -dependence.²⁷ At $(\lambda\tau_q)^{-1} \sim \hbar/K$, the result thereby obtained are identical to Eq. (83). This reflects a basic belief previously anticipated.^{27,28,44} That is, a physical regularizer strength must match the minimal quantum wave packet.

¹D. M. Basko, M. A. Skvortsov, and V. E. Kravtsov, Phys. Rev. Lett. **90**, 096801 (2003); V. E. Kravtsov, cond-mat/0312316.

²F. L. Moore, J. C. Robinson, C. F. Bharucha, Bala Sundaram, and M. G. Raizen, Phys. Rev. Lett. **75**, 4598 (1995); C. F. Bharucha, J. C. Robinson, F. L. Moore, Bala Sundaram, Q. Niu, and M. G. Raizen, Phys. Rev. E **60**, 3881 (1999).

³M. G. Raizen, Adv. At., Mol., Opt. Phys. **41**, 43 (1999).

⁴C. Zhang, J. Liu, M. G. Raizen, and Q. Niu, Phys. Rev. Lett. **92**, 054101 (2004).

⁵O. A. Starykh, P. R. J. Jacquod, E. E. Narimanov, and A. D. Stone, Phys. Rev. E **62**, 2078 (2000).

⁶G. Casati, B. V. Chirikov, J. Ford, and F. M. Izrailev, in *Stochastic Behavior of Classical and Quantum Hamiltonian Systems*, Lecture Notes in Physics 93, edited by G. Casati and J. Ford (Springer, New York, 1979).

⁷B. V. Chirikov, F. M. Izrailev, and D. L. Shepelyansky, Sov. Sci. Rev., Sect. C, Math. Phys. Rev. **2**, 209 (1981).

⁸H. Ammann, R. Gray, I. Shvarchuck, and N. Christensen, Phys. Rev. Lett. **80**, 4111 (1998).

⁹B. V. Chirikov, Phys. Rep. **52**, 263 (1979).

¹⁰A. L. Lichtenberg and M. A. Lieberman, *Regular and Chaotic Dynamics* (Springer-Verlag, Berlin, 1991).

¹¹A. B. Rechester and R. B. White, Phys. Rev. Lett. **44**, 1586 (1980); A. B. Rechester, M. N. Rosenbluth, and R. B. White, Phys. Rev. A **23**, 2664 (1981).

¹²M. Khodas and S. Fishman, Phys. Rev. Lett. **84**, 2837 (2000); Erratum, *ibid.* **84**, 5918 (2000); M. Khodas, S. Fishman, and O. Agam, Phys. Rev. E **62**, 4769 (2000).

¹³S. Fishman, D. R. Grempel, and R. E. Prange, Phys. Rev. Lett. **49**, 509 (1982).

- ¹⁴D. R. Grempel, R. E. Prange, and S. Fishman, *Phys. Rev. A* **29**, 1639 (1984).
- ¹⁵R. Blümel and U. Smilansky, *Phys. Rev. Lett.* **69**, 217 (1992).
- ¹⁶P. A. Lee and T. V. Ramakrishnan, *Rev. Mod. Phys.* **57**, 287 (1985).
- ¹⁷L. P. Gorkov, A. I. Larkin, and D. E. Khmel'nitskii, *Pis'ma Zh. Eksp. Teor. Fiz.* **30**, 248 (1979) [*JETP Lett.* **30**, 248 (1979)].
- ¹⁸A. Altland, *Phys. Rev. Lett.* **71**, 69 (1993).
- ¹⁹A. Altland and M. R. Zirnbauer, *Phys. Rev. Lett.* **77**, 4536 (1996); **80**, 641 (1998); G. Casati, F. M. Izrailev, and V. V. Sokolov, *ibid.* **80**, 640 (1998).
- ²⁰K. Efetov, *Supersymmetry in Disorder and Chaos* (Cambridge University Press, Cambridge, UK, 1997).
- ²¹A. I. Larkin and Yu. N. Ovchinnikov, *Zh. Eksp. Teor. Fiz.* **55**, 2262 (1968) [*Sov. Phys. JETP* **28**, 1200 (1969)].
- ²²G. P. Berman and G. M. Zaslavsky, *Physica A* **91**, 450 (1978); G. M. Zaslavsky, *Phys. Rep.* **80**, 157 (1981).
- ²³For a review, see F. M. Izrailev, *Phys. Rep.* **196**, 299 (1990).
- ²⁴Ph. Jacquod and E. V. Sukhorukov, *Phys. Rev. Lett.* **92**, 116801 (2004); J. Tworzydło, A. Tajic, and C. W. J. Beenakker, *Phys. Rev. B* **69**, 165318 (2004).
- ²⁵M. C. Goorden, Ph. Jacquod, and C. W. J. Beenakker, *Phys. Rev. B* **68**, 220501(R) (2003).
- ²⁶J. Tworzydło, A. Tajic, H. Schomerus, and C. W. J. Beenakker, *Phys. Rev. B* **68**, 115313 (2003); P. G. Silvestrov, M. C. Goorden, and C. W. J. Beenakker, *Phys. Rev. Lett.* **90**, 116801 (2003).
- ²⁷I. L. Aleiner and A. I. Larkin, *Phys. Rev. B* **54**, 14423 (1996).
- ²⁸M. G. Vavilov and A. I. Larkin, *Phys. Rev. B* **67**, 115335 (2003).
- ²⁹C. Tian, A. Kamenev, and A. I. Larkin, *Phys. Rev. Lett.* **93**, 124101 (2004).
- ³⁰J. Müller and A. Altland, *J. Phys. A* **38**, 3097 (2005).
- ³¹D. L. Shepelyansky, *Physica D* **28**, 103 (1987).
- ³²D. A. Steck, V. Milner, W. H. Oskay, and M. G. Raizen, *Phys. Rev. E* **62**, 3461 (2000).
- ³³P. H. Jones, M. Stocklin, G. Hur, and T. S. Monteiro, *Phys. Rev. Lett.* **93**, 223002 (2004); P. H. Jones, M. Goonasekera, H. E. Saunders-Singer, and D. R. Meacher, *quant-ph/0309149*.
- ³⁴S. Montangero, A. Romito, G. Benenti, and R. Fazio, *cond-mat/0407274*.
- ³⁵A. Isacsson, L. Y. Gorelik, R. I. Shekhter, Y. M. Galperin, and M. Jonson, *Phys. Rev. Lett.* **89**, 277002 (2002); L. Y. Gorelik, A. Isacsson, Y. M. Galperin, R. I. Shekhter, and M. Jonson, *Nature (London)* **411**, 454 (2001).
- ³⁶S. Hikami, *Phys. Rev. B* **24**, 2671 (1981).
- ³⁷M. R. Zirnbauer, in *Supersymmetry and Trace Formulae, Chaos and Disorder*, edited by I. V. Lerner, J. P. Keating, and D. E. Khmel'nitskii (Kluwer Academic/Plenum, New York, 1999).
- ³⁸See, e.g., G. M. Zaslavsky, M. Edelman, and B. A. Niyazov, *Chaos* **7**, 159 (1997).
- ³⁹F. M. Izrailev, *Phys. Rev. Lett.* **56**, 541 (1986).
- ⁴⁰M. Thaha, R. Blümel, and U. Smilansky, *Phys. Rev. E* **48**, 1764 (1993).
- ⁴¹T. Tworzydło, A. Tajic, and C. W. J. Beenakker, *Phys. Rev. B* **70**, 205324 (2004).
- ⁴²R. A. Smith, I. V. Lerner, and B. L. Altshuler, *Phys. Rev. B* **58**, 10343 (1998).
- ⁴³R. S. Whitney, I. V. Lerner, and R. A. Smith, *Waves Random Media* **9**, 179 (1999).
- ⁴⁴C. Tian and A. I. Larkin, *Phys. Rev. B* **70**, 035305 (2004).
- ⁴⁵For a review see, e.g., S. Chu, *Science* **253**, 861 (1991); W. D. Phillips, *Rev. Mod. Phys.* **70**, 721 (1998); C. E. Wieman, D. E. Pritchard, and D. J. Wineland, *ibid.* **71**, S253 (1999).
- ⁴⁶R. Graham, M. Schlautmann, and P. Zoller, *Phys. Rev. A* **45**, R19 (1992).
- ⁴⁷F. L. Moore, J. C. Robinson, C. Bharucha, P. E. Williams, and M. G. Raizen, *Phys. Rev. Lett.* **73**, 2974 (1994); J. C. Robinson, C. Bharucha, F. L. Moore, R. Jahnke, G. A. Georgakis, Q. Niu, M. G. Raizen, and Bala Sundaram, *ibid.* **74**, 3963 (1995).
- ⁴⁸In the conventional QKR is periodic, i.e., $\Psi(\theta+2\pi)=\Psi(\theta)$, leading to the discrete angular momentum: $l=n\hbar$ with n integer. Periodically kicked cold atomic gases differ from it, with the boundary condition replaced by $\Psi(\theta+2\pi)=\Psi(\theta)e^{i\theta l_0}$, where $l_0 \in [0, 1]$ is a fractional part of an atom's momentum in units $2\hbar k_L$. It may be eliminated by the gauge transformation that introduces an Aharonov-Bohm flux into the kinetic energy ($\hat{l}-l_0$)²/2. Such flux does not affect dynamical localization, though quantum resonances (Ref. 23) is eliminated by averaging over l_0 .
- ⁴⁹C. Tian, A. Kamenev, and A. I. Larkin, *Bull. Am. Phys. Soc.* **49**, 482 (2004).
- ⁵⁰E. Chow, P. Delsing, and D. B. Haviland, *Phys. Rev. Lett.* **81**, 204 (1998).
- ⁵¹D. B. Haviland and P. Delsing, *Phys. Rev. B* **54**, R6857 (1996).
- ⁵²M. Watanabe and D. B. Haviland, in *Studies of High Temperature Superconductors (Advances in Research and Applications)*, edited by A. Narlikar (Nova Science Publishers, New York, 2002), Vol. 43.
- ⁵³D. Cohen, *Phys. Rev. A* **44**, 2292 (1991).
- ⁵⁴V. Milner, D. A. Steck, W. H. Oskay, and M. G. Raizen, *Phys. Rev. E* **61**, 7223 (2000).
- ⁵⁵B. G. Klappauf, W. H. Oskay, D. A. Steck, and M. G. Raizen, *Phys. Rev. Lett.* **81**, 1203 (1998).
- ⁵⁶M. B. d'Arcy, R. M. Godun, G. S. Summy, I. Guarneri, S. Wimberger, S. Fishman, and A. Buchleitner, *Phys. Rev. E* **69**, 027201 (2004).
- ⁵⁷S. Jitomirskaya, *Proceedings of the ICM, Beijing 2002*, Vol. 3, p. 445; J. Bourgain and S. Jitomirskaya (unpublished); S. Jitomirskaya, private communication.
- ⁵⁸S. Wimberger, I. Guarneri, and S. Fishman, *Nonlinearity* **16**, 1381 (2003).
- ⁵⁹S. Fishman, I. Guarneri, and L. Rebuzzini, *Phys. Rev. Lett.* **89**, 084101 (2002).
- ⁶⁰C. Tian and A. I. Larkin, *cond-mat/0503333*.
- ⁶¹I. L. Aleiner and A. I. Larkin, *Phys. Rev. E* **55**, R1243 (1997).
- ⁶²A. J. Daley and A. S. Parkins, *Phys. Rev. E* **66**, 056210 (2002); G. Duffy, S. Parkins, T. Muller, M. Sadgrove, R. Leonhardt, and A. C. Wilson, *ibid.* **70**, 056206 (2004).
- ⁶³K. B. Efetov, G. Schwiete, and K. Takahashi, *Phys. Rev. Lett.* **92**, 026807 (2004).